Article

Cell Reports

Differential Roles of the mTOR-STAT3 Signaling in Dermal γδ T Cell Effector Function in Skin Inflammation

Graphical Abstract

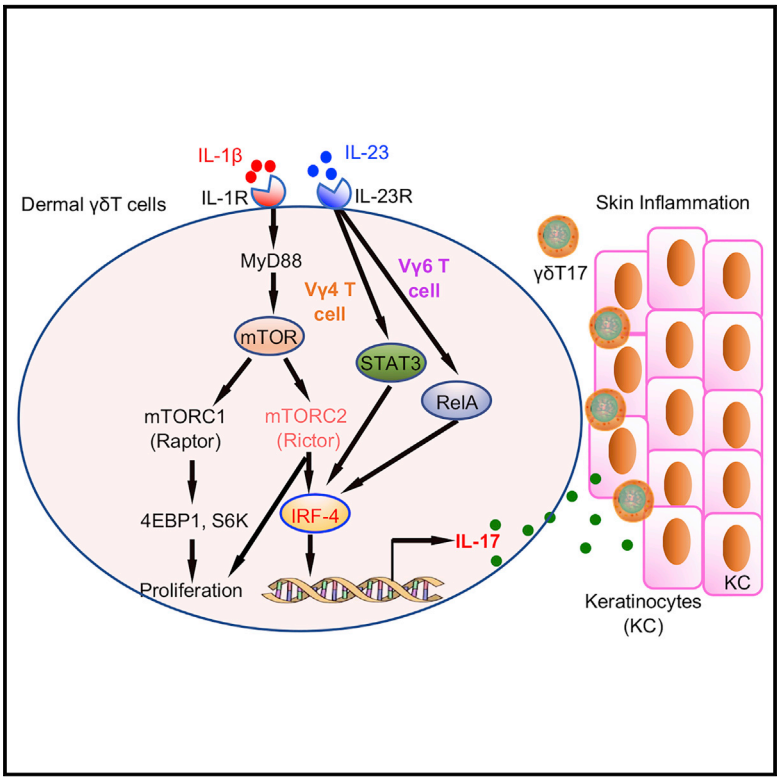

Authors

Yihua Cai, Feng Xue, Hui Qin, ..., Fuxiang Chen, Jie Zheng, Jun Yan

Correspondence

jun.yan@louisville.edu

In Brief

Cai et al. demonstrate that the mTOR and STAT3 signaling pathways differentially regulate dermal Vγ4 and Vγ6 T cell effector function, leading to distinct outcomes in skin inflammation.

Highlights

- Dermal gamma-delta T cell effector function relies on IL-1R and IL-23R pathways
- mTORC2 is essential for dermal gamma-delta T17 cell function and skin inflammation
- STAT3 signaling is critical for dermal Vγ4 T cell function, but not for Vγ6 T cells
- IRF-4 links IL-1β and IL-23 signaling for dermal gamma-delta T cell IL-17 production

Cai et al., 2019, Cell Reports 27, 3034–3048
June 4, 2019
https://doi.org/10.1016/j.celrep.2019.05.019

CellPress

OPEN ACCESS
CellPress

Cell Reports
Article

Differential Roles of the mTOR-STAT3 Signaling in Dermal γδ T Cell Effector Function in Skin Inflammation

Yihua Cai,[1,4] Feng Xue,[2,4] Hui Qin,[1,2,4] Xu Chen,[1,3] Na Liu,[2] Chris Fleming,[1] Xiaoling Hu,[1] Huang-ge Zhang,[1] Fuxiang Chen,[3] Jie Zheng,[2] and Jun Yan[1,5,*]

[1]Department of Medicine and Department of Microbiology and Immunology, James Graham Brown Cancer Center, University of Louisville, Louisville, KY, USA

[2]Department of Dermatology, Ruijin Hospital, School of Medicine, Shanghai Jiaotong University, Shanghai, P.R. China

[3]Department of Laboratory Medicine, Shanghai Ninth People's Hospital, Shanghai Jiaotong University School of Medicine, Shanghai, P.R. China

[4]These authors contributed equally

[5]Lead Contact

*Correspondence: jun.yan@louisville.edu

https://doi.org/10.1016/j.celrep.2019.05.019

SUMMARY

Dermal γδT cells play critical roles in skin homeostasis and inflammation. However, the underlying molecular mechanisms by which these cells are activated have not been fully understood. Here, we show that the mechanistic or mammalian target of rapamycin (mTOR) and STAT3 pathways are activated in dermal γδT cells in response to innate stimuli such as interleukin-1β (IL-1β) and IL-23. Although both mTOR complex 1 (mTORC1) and mTORC2 are essential for dermal γδT cell proliferation, mTORC2 deficiency leads to decreased dermal γδT17 cells. It appears that mitochondria-mediated oxidative phosphorylation is critical in this process. Notably, although the STAT3 pathway is critical for dermal Vγ4T17 effector function, it is not required for Vγ6T17 cells. Transcription factor IRF-4 activation promotes dermal γδT cell IL-17 production by linking IL-1β and IL-23 signaling. The absence of mTORC2 in dermal γδT cells, but not STAT3, ameliorates skin inflammation. Taken together, our results demonstrate that the mTOR-STAT3 signaling differentially regulates dermal γδT cell effector function in skin inflammation.

INTRODUCTION

The skin is a crucial immunological organ and acts as a first line of physical and immunological defense. Interleukin-17 (IL-17) and its family cytokines have been shown to be essential in controlling this process. Although the cellular sources of IL-17 have been increasingly added, we and others have demonstrated that innate, dermal γδT cells are the major IL-17 producers (γδT17) in the skin and play an essential role in skin inflammation (Cai et al., 2011; Sumaria et al., 2011). The critical role of dermal γδT17 cells in skin inflammation has been further demonstrated by many other studies (Gatzka et al., 2013; Kulig et al., 2016; Mabuchi et al., 2011; Pantelyushin et al., 2012; Riol-Blanco et al., 2014; Yoshiki et al., 2014). We have also shown that dermal γδT17 cells have a unique developmental requirement, which is different from γδT cells from other anatomical sites (Cai et al., 2014). However, the underlying factors that regulate dermal γδT17 cells in the steady condition and skin inflammation have not been fully defined. Previous studies have shown that cytokines IL-1β and IL-23 stimulate γδ T cells for IL-17 production (Sutton et al., 2009) and promote γδT17 cell development from peripheral $CD27^{+}CD122^{-}$ γδT cells (Muschaweckh et al., 2017). IL-23 has also been shown to drive peripheral γδT17 cell differentiation and expansion (Papotto et al., 2017). Additionally, cytokine IL-7 can promote mouse and human γδT17 expansion (Michel et al., 2012). Certain pathogens also directly interact with γδT cells to induce IL-17 production (Martin et al., 2009). Besides innate stimuli, activation of TCR signaling on γδT cells further enhances cytokine-induced IL-17 production from γδT cells (Michel et al., 2012; Sutton et al., 2009; Zeng et al., 2012). Despite these progresses made with γδT17 cells, little is known about the molecular pathways that regulate dermal γδT17 cell effector function.

The mechanistic or mammalian target of rapamycin (mTOR) signaling pathway plays a critical role in T cell proliferation, differentiation, and effector functions (Laplante and Sabatini, 2012; Zeng and Chi, 2013; Zeng et al., 2013). The serine and/or threonine kinase mTOR consists of two distinct complexes: mTOR complex 1 (mTORC1) and 2 (mTORC2). The Raptor (regulatory associated protein of mTOR) is associated with mTORC1, whereas Rictor (rapamycin-insensitive companion of mTOR) is part of complex mTORC2. The ribosomal p70S6 kinase (p70S6K) and the 4E-binding protein 1 (4EBP1) are downstream of mTORC1 and mTORC2 controls AKT, SGK1, and protein kinase Cα (PKCα). Recent studies have demonstrated that the phosphatidylinositol 3-kinase (PI3K)-AKT-mTORC1-S6K axis positively regulates Th17 cell differentiation by promoting transcription factor RORγt nuclear translocation (Kim et al., 2014; Kurebayashi et al., 2012). In addition, the mTOR signaling

pathway plays a role in the proliferation of epidermal keratinocytes and angiogenesis (Huang et al., 2014; Raychaudhuri and Raychaudhuri, 2014), hallmarks of psoriasis pathogenesis. Recent studies also show that lack of mTORC1 promotes γδT cell generation (Yang et al., 2018), and transcription factor c-Maf is essential for γδT17 cell differentiation and maintenance (Zuberbuehler et al., 2019). In the case of skin wound healing, inhibition of the mTOR pathway by rapamycin treatment suppresses proliferation of resident γδT cells, but not keratinocytes (Mills et al., 2008). However, it is unknown whether the mTOR pathway regulates dermal γδT cells, particularly dermal γδT17 cells in skin inflammation.

In the current study, we investigate the signaling pathways that are essential in dermal γδT17 cell effector function. We show that both IL-1R and IL-23R pathways are needed for dermal γδT17 cell activation, although IL-1R is also critically involved in dermal γδT17 cell expansion. Mechanistically, IL-1β activates the mTOR signaling pathway via IL-1R-MyD88, whereas IL-23 activates the STAT3 pathway. Further studies show that although both mTORC1 and mTORC2 are critical in dermal γδT17 cell expansion, IL-17 production in dermal γδT cells is abrogated in mTORC2-deficient mice. This is associated with increased dysfunctional mitochondria and mitochondria reactive oxygen species (ROS) production. On the contrary, IL-23 stimulates STAT3 activation, which is critical in dermal Vγ4 effector function, whereas dermal Vγ6 effector function is independent of the STAT3 pathway. Transcription factor IRF-4 appears to link the IL-1R and IL-23R pathways to induce enhanced IL-17 production in dermal γδ T cells. Consequently, skin inflammation is drastically reduced in mTORC2-deficient mice, but not in STAT3-deficient mice. Thus, our study reveals a critical molecular mechanism by which dermal γδ T cells are activated for effector function.

RESULTS

Dermal γδT Cell IL-17 Production and Expansion Require IL-1R and IL-23R Signaling Pathways

Psoriasis is an autoinflammatory skin disease affecting approximately 2% of the population worldwide. Inflammatory cytokines including IL-23 and IL-1 have been shown to be critical in regulating disease pathogenesis (Di Meglio et al., 2014). We used RNA-based next-generation sequencing (RNA-seq) to analyze lesional skin samples from psoriasis patients effectively treated with glucocorticoid. Gene set enrichment analysis (GSEA) revealed that regulation of IL-12 production genes, including IL-23 and IL-23R, and IL-1R signaling pathway-related genes was downregulated in patients effectively treated with glucocorticoid (Figure 1A), suggesting that these two pathways are related to not only disease pathogenesis but also treatment response. Previous studies have shown that cytokine IL-17 plays a critical role in psoriasis pathogenesis (Lowes et al., 2014), IL-1β and IL-23 are essential to promote extrathymic commitment of γδT17 cells (Muschaweckh et al., 2017), and IL-23 drives peripheral γδT17 differentiation (Papotto et al., 2017). In mouse skin, dermal γδT cells are the major cellular source of IL-17 and play a critical role in skin inflammation. Therefore, we examined dermal γδT cell response upon IL-1β and IL-23 stimulation. Combined IL-1β and IL-23 indeed induced enhanced IL-17 production in dermal γδT cells (Figure S1). This was the case for both dermal Vγ4 and Vγ6 T cells (Figure 1B), two main subsets of γδT cells in the skin (Cai et al., 2014). The IL-17 production from dermal γδT cells including Vγ4 and Vγ6 T cells was significantly reduced in IL-1R or IL-23R knockout (KO) mice (Figure S1; Figures 1B and 1C). We next examined dermal γδT cell *in vitro* expansion in the presence of IL-1β and/or IL-23. Although IL-23 alone stimulated dermal γδ T cell proliferation, this effect was abrogated in IL-1R KO mice, whereas IL-1β-induced dermal γδT cell proliferation was only partly diminished in IL-23R KO mice (Figure S1; Figure 1D), suggesting a differential signaling requirement for dermal γδT cell expansion. This was particularly the case for dermal Vγ4 T cells (Figures 1B and 1D).

IL-1β Stimulates Dermal γδT Cell Proliferation and IL-17 Production via the mTOR Signaling Pathway

Because the IL-1β/IL-1R axis is critical in dermal γδT cell expansion and IL-17 production, we next examined the underlying molecular mechanism by which IL-1β induces dermal γδT cell effector function. Dermal γδT cells constitutively expressed p-mTOR, but not p-STAT3, as assessed by Phosflow analysis (Figure 2A). IL-1β stimulation enhanced phosphorylation of mTOR, whereas IL-23 induced STAT3 activation in dermal γδT cells. This was also confirmed by western blot analysis (Figure 2B) and confocal microscopy (Figure 2C). Combined IL-1β with IL-23 did not show enhanced p-mTOR or p-STAT3 (Figure 2B). Notably, IL-1β-induced p-mTOR expression was completely abrogated in IL-1R KO mice, but not drastically altered in IL-23R KO mice, whereas IL-23-induced p-STAT3 was not changed in IL-1R KO mice but was abrogated in IL-23R KO mice (Figure 2D). To investigate whether indeed the mTOR signaling plays a critical role in dermal γδT cell function, skin cells were labeled with carboxyfluorescein succinimidyl ester (CFSE) and stimulated with IL-1β and IL-23 in the presence or absence of the mTOR inhibitor rapamycin. As depicted in Figure 2E, rapamycin treatment significantly decreased dermal γδT cell *in vitro* proliferation and IL-17 production induced by IL-1β and IL-23.

mTORC2 Is Critical in IL-1β-Induced Dermal γδT Cell Effector Function

The mTOR exists in two distinct complexes, mTORC1 and mTORC2, which contain scaffold protein Raptor or Rictor, respectively. mTORC1 induces phosphorylation of 4E-BP1 and p70-S6 kinase leading to transcriptional regulation (Inoki et al., 2005), whereas mTORC2 induces phosphorylation and feedback activation of AKT (Sarbassov et al., 2005). Previous studies have shown that mTORC1 and mTORC2 have distinct functions in directing CD4 T cell differentiation and function (Lee et al., 2010). Although mTORC1 is sensitive to rapamycin, mTORC2 can also be inhibited by a prolonged or high dose of rapamycin in CD4 T cells (Delgoffe et al., 2011; Sarbassov et al., 2006). Therefore, we examined mTORC1 and mTORC2 activation in dermal γδT cells. IL-1β-induced phosphorylation of AKT and S6 was revealed by western blot analysis (Figure 3A). This was also confirmed by Phosflow analysis (Figure 3B). We next used CD2-cre;Raptor$^{fl/fl}$ and Rictor$^{fl/fl}$ mice to assess relative

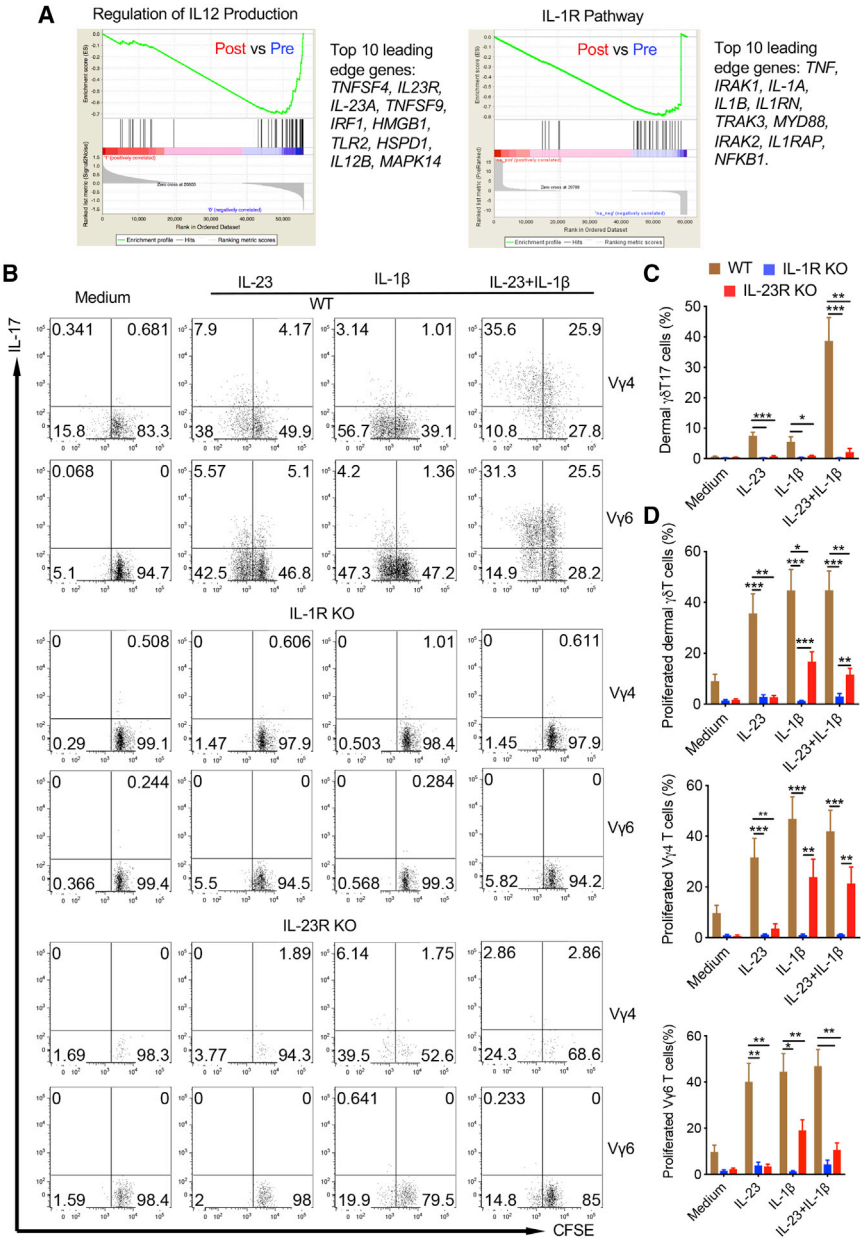

Figure 1. Dermal γδT Cell Activation Requires Both IL-1R and IL-23R Signaling Pathways

(A) Gene set enrichment analysis identifies transcriptional downregulation of the IL-12 production regulatory pathway and IL-1R pathway in psoriasis patients effectively treated with glucocorticoid. The top 10 leading edge genes in these two pathways are shown.

(B) Whole skin cell suspensions from WT, IL-1R KO, and IL-23R KO mice were labeled with CFSE and stimulated with IL-23, IL-1β, or IL-23 plus IL-1β for 3 days. Cell proliferation and intracellular IL-17 were analyzed by flow cytometry. Flow plots gated on $CD3^+\gamma\delta TCR^{int}V\gamma4$ or $CD3^+\gamma\delta TCR^{int}V\gamma6$ cells are representative of at least two independent experiments with similar results. Each experiment includes at least three mice from WT, IL-1R KO, or IL-23R KO strains.

(C) Summarized percentages of dermal γδT17 cells are shown as mean ± SEM. *$p < 0.05$, **$p < 0.01$, ***$p < 0.001$ (unpaired Student's t test).

(D) Summarized dermal γδT cell proliferation with different subsets of dermal γδT cells (Vγ4 and Vγ6) is shown as mean ± SEM. *$p < 0.05$, **$p < 0.01$, ***$p < 0.001$ (unpaired Student's t test).

contributions of mTORC1 and mTORC2 in dermal γδT cell effector function. In CD2-cre;$Raptor^{fl/fl}$ mice, the overall T cells in the skin including αβT cells, dermal γδT cells, and epidermal γδT cells were not significantly altered compared with control mice, although dermal Vγ4 T cells were decreased, whereas Vγ6 T cells were increased (Figure S2A). In contrast, these mice had increased $CD3^+$ T cells and γδT cells and decreased Vγ4, but increased Vγ6 in the peripheral lymph nodes (Figure S2B), suggesting that mTORC1 plays a critical role in peripheral γδT cell homeostasis. Deletion of Raptor in dermal γδT cells abrogated phosphor-S6 activation by IL-1β stimulation (Figure S3A). Dermal γδT cells showed significantly decreased *in vitro* proliferation upon IL-1β stimulation in *CD2-cre; $Raptor^{f/f}$* mice (Figure S3B). However, dermal γδT cell IL-17 production in *CD2-cre; $Raptor^{f/f}$* mice was not affected (Figure S3C).

Similarly, different T cell subsets in the skin of CD2-cre;$Rictor^{fl/fl}$ and $Rictor^{fl/fl}$ mice were not significantly altered, although dermal Vγ4 T cells were decreased whereas Vγ6 T cells were increased in Rictor conditional KO (cKO) mice (Figure S2C). Rictor cKO mice also had increased γδT cells, although both Vγ4 and Vγ6 were decreased, but Vγ1 increased in the peripheral lymph nodes (Figure S2D). Deletion of Rictor in dermal γδT cells abrogated phosphor-AKT activation upon IL-1β stimulation (Figure 3C). Dermal γδT cell proliferation and IL-17 production were significantly diminished in *CD2-cre; $Rictor^{f/f}$* mice (Figures 3D and 3E) upon IL-1β or IL-1β plus IL-23 stimulation. This was for both Vγ4 and Vγ6 T cells (data not shown). The gating strategy was shown in Figure S3D. However, IL-23-induced STAT3 phosphorylation was not affected in *CD2-cre; $Rictor^{f/f}$* or *$Raptor^{f/f}$* mice (Figure 3F), suggesting that mTORC2 is essential in IL-1β-induced dermal γδT cell effector function.

MyD88 Is Required for IL-1β-Induced mTOR Activation in Dermal γδT Cells

Previous studies have shown that MyD88 is essential to sustain the mTOR activity, thus promoting Th17 cell proliferation (Chang et al., 2013). In addition, IL-1β promotes granulocyte-macrophage

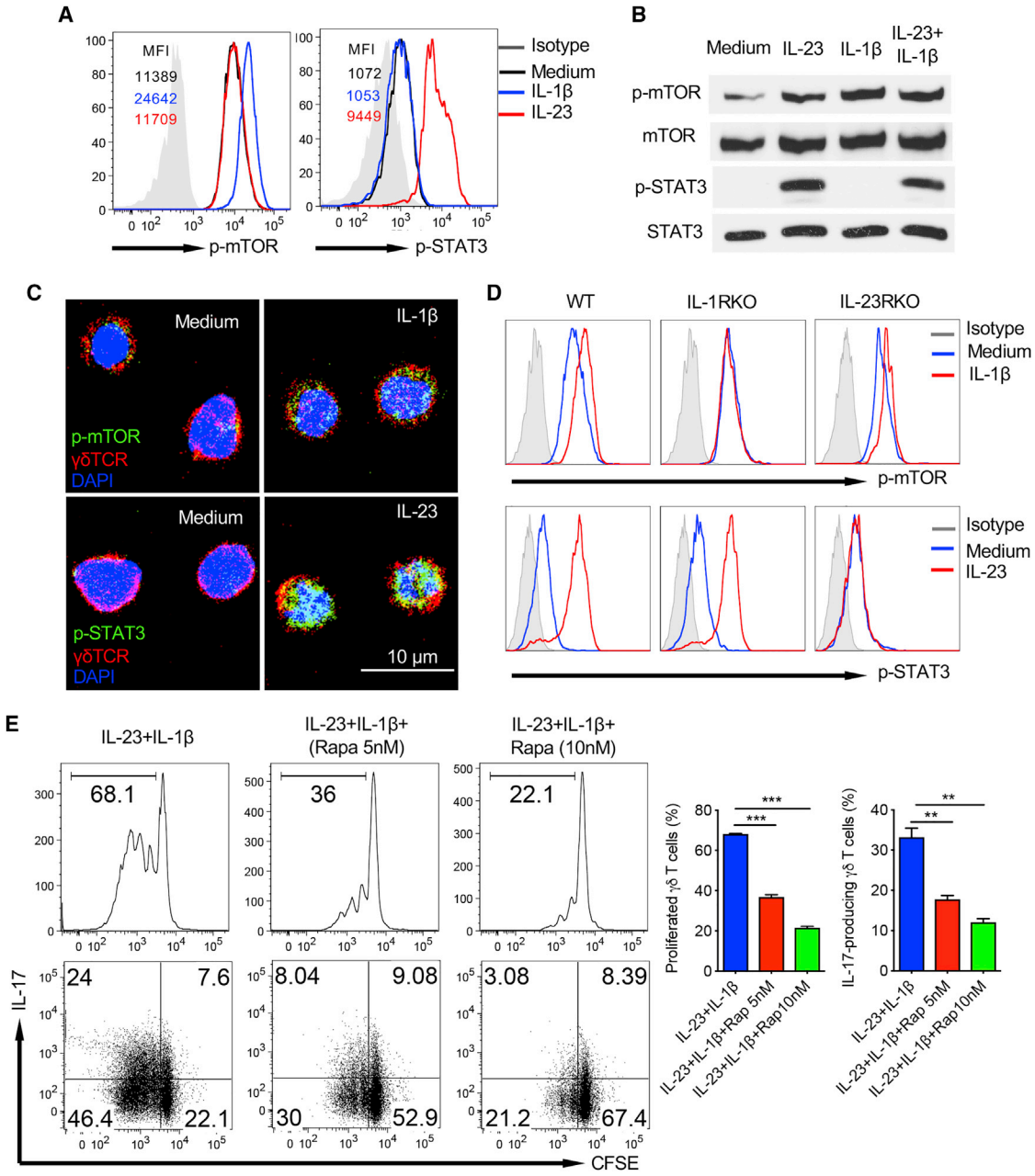

Figure 2. IL-1β-Induced Dermal γδ T Cell Activation Is Dependent on the mTOR-Mediated Signaling Pathway

(A and B) Cultured skin γδT cell lines from C57BL/6 WT mice were stimulated with IL-23 and/or IL-1β for 30 min. p-STAT3 and p-mTOR were examined by flow cytometry (A) or western blot (B) analysis. Flow histograms gated on $CD3^+\gamma\delta TCR^+$ cells are representative of at least three independent experiments with similar results. Each experiment includes at least two mice. Western blot analysis is representative of two independent experiments with similar results.

(C) $CD45^+CD4^-CD8^-$ cells were sorted from cultured C57BL/6 WT skin γδT cell lines and then stimulated with IL-23 or IL-1β for 30 min. Cells were stained with fluorochrome-labeled γδTCR (red) and p-mTOR (green) or p-STAT3 (green) with DAPI (blue). Representative images are shown. Scale bar: 10 μm.

(D) Cultured skin γδT cell lines from WT, IL-1R KO, and IL-23R KO mice were stimulated with IL-23 or IL-1β for 30 min. p-STAT3 and p-mTOR were examined by flow cytometry. Flow histograms gated on $CD3^+\gamma\delta TCR^+$ cells are representative of at least two independent experiments with similar results. Each experiment includes at least three mice from WT, IL-1R KO, or IL-23R KO strains.

(E) Whole skin cell suspensions from WT mice were labeled with CFSE and then stimulated with IL-23 plus IL-1β in the presence or absence of rapamycin for 3 days. CFSE dilution and intracellular IL-17 production by dermal γδT cells were determined by flow cytometry. Flow plots gated on $CD3^+\gamma\delta TCR^{int}$ cells are representative of at least three independent experiments with similar results. Each experiment includes at least three C57BL/6 WT mice. Proliferated dermal γδT cells and percentages of IL-17-producing γδT cells are shown as mean ± SD. $^{**}p < 0.01$, $^{***}p < 0.001$ (one-way ANOVA).

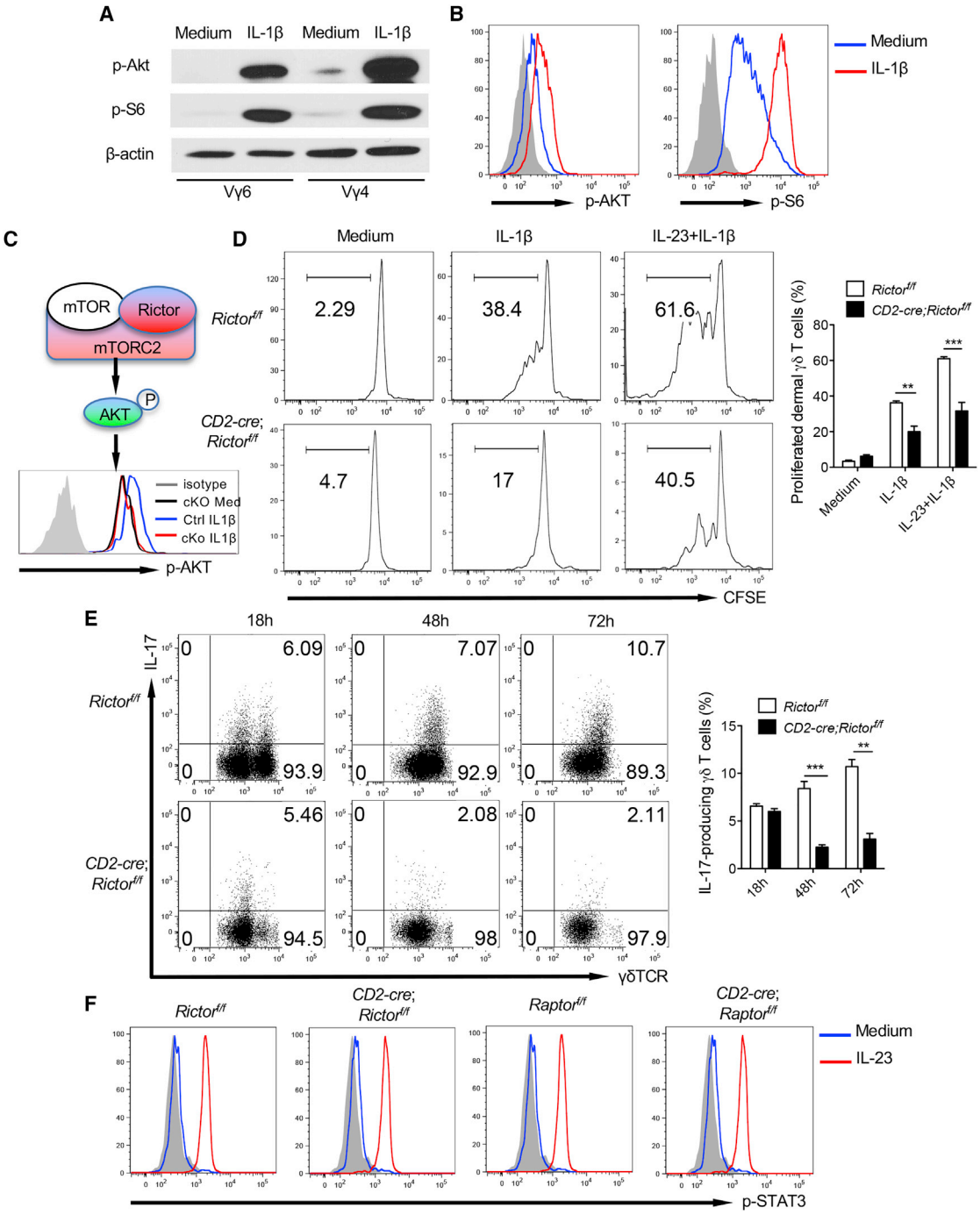

Figure 3. mTORC2-Mediated Signaling Pathway Is Critical in IL-1β-Induced Dermal γδT Cell Activation

(A and B) Sorted Vγ6 (Vγ4^{-}) or Vγ4 T cells from cultured skin γδT cell lines were stimulated with IL-1β for 30 min. p-AKT and p-S6 were examined by western blot (A) or flow cytometry (B). Western blot analysis is representative of two independent experiments with similar results. Flow histograms gated on CD3^{+}γδTCR^{+} cells are representative of at least three independent experiments with similar results. Each experiment includes at least two WT mice.

(C) Schematic of mTORC2 with representative histogram showing abolished mTORC2 activity (p-AKT) in Rictor-deficient dermal γδT cells upon IL-1β stimulation. Flow histogram was gated on CD3^{+}γδTCR^{+} cells.

(D) Whole skin cell suspensions from CD2-cre;Rictor$^{f/f}$ or control Rictor$^{f/f}$ mice were labeled with CFSE and then stimulated with IL-1β or IL-23 plus IL-1β for 3 days. CFSE dilution by dermal γδT cells was determined by flow cytometry. Flow plots gated on CD3^{+}γδTCR^{int} cells are representative of at least three independent experiments with similar results. Each experiment includes at least two mice from CD2-cre;Rictor$^{f/f}$ or control Rictor$^{f/f}$ strains. Proliferated dermal γδ T cells are shown as mean ± SEM. **p < 0.01, ***p < 0.001 (unpaired Student's t test).

(legend continued on next page)

colony-stimulating factor (GM-CSF) production in αβ and γδT cells via MyD88 (Lukens et al., 2012). To further delineate the possible role of MyD88 in IL-17-producing dermal γδT cell differentiation and activation, we first examined dermal γδT cells from MyD88 KO mice and IL-1R KO mice. Notably, dermal γδT cell frequency was not altered in IL-1R KO mice but was significantly decreased in MyD88 KO mice (Figure S4A). In addition, IL-17-producing dermal γδT cells were decreased in both IL-1R KO and MyD88 KO mice. We next examined dermal γδT cell proliferation and IL-17 production upon IL-1β or IL-1β plus IL-23 stimulation. As shown in Figure S4B, IL-1β-induced dermal γδT cell proliferation and IL-17 production were completely abrogated in MyD88 KO mice. Further Phosflow analysis revealed that IL-23-induced STAT3 phosphorylation was not impaired in IL-1R KO or MyD88 KO mice (Figure S4C). In contrast, IL-1β-induced phosphorylation of AKT and S6 was completely abrogated in IL-1R and MyD88 KO mice, suggesting that IL-1β-induced mTOR activation requires MyD88, whereas IL-23-induced STAT3 activation is independent on the IL-1R-MyD88 pathway.

mTORC2 Deficiency Induces Accumulation of Dysfunctional Mitochondria

Because mTOR signaling plays a critical role in cellular metabolism, we reasoned that the abrogated IL-17 production and proliferation in mTORC2-deficient γδT cells may be caused by altered metabolic profiles. IL-17-producing γδT cells predominately used an oxidative phosphorylation pathway for energy fuel because inhibition of isocitrate dehydrogenase (IDH) by AGI and pyruvate kinase (PK) by oxalate (OXA) significantly diminished IL-17 production from γδT cells (Figure 4A). 2-Deoxyglucose (2-DG) acts to competitively inhibit glycolysis. Addition of 2-DG, however, showed no impact on IL-17 production. We then examined enzymes that are related to glucose metabolism, and found no substantial differences between Rictor cKO and control mice (Figure 4B). Furthermore, we did not find differences of glucose uptake among Raptor or Rictor cKO mice and corresponding control mice as measured by 2-2-(N-(7-nitrobenz-2-oxa-1,3-diazol-4-yl)amino)-2-deoxyglucose (NBDG) staining (Figure 4C). 2-NBDG is a fluorescent glucose analog that has been used to determine glucose uptake. We next investigated whether the altered metabolic profiles of mitochondria are responsible for the deceased IL-17 production in Rictor cKO dermal γδT cells. We stained dermal γδT cells with MitoTracker Green and MitoTracker Red to distinguish between respiring mitochondria (MitoTracker Red^{+}) and dysfunctional mitochondria (MitoTracker Green$^{+/high}$, MitoTracker Red$^{+/low}$) (Ip et al., 2017). We observed an increase in dysfunctional mitochondria but decrease in respiring mitochondria in Rictor cKO dermal γδT cells compared with those in control mice (Figure 4D). However, no differences were noted in Raptor cKO dermal γδT cells (Figure 4D). These data suggest that decreased respiring mitochondria may account for the decreased IL-17 production in Rictor cKO dermal γδT cells.

Loss of mitochondria membrane potential (ΔΨm) is associated with accumulation of mitochondrial ROS. We thus examined whether accumulation of dysfunctional mitochondria (ΔΨm^{low}) in Rictor cKO dermal γδ T cells was associated with production of mitochondrial ROS. To assess ROS levels in the mitochondria, we used the mitochondria-specific ROS indicator MitoSOX to detect superoxide in the mitochondria of live cells. We found that MitoSOX-positive cells were significantly higher in Rictor-deficient dermal γδT cells than those in control mice (Figure 4E). In addition, the overall ROS production determined by 2′,7′-dichlorodihydrofluorescein diacetate (DCFDA) assay in dermal γδT cells from Rictor cKO mice was also higher than control mice (Figure 4F). To further support this notion, we found that addition of the ROS inhibitor N-acetylcysteine (NAC) could rescue IL-17 production by dermal γδT cells from Rictor cKO mice (Figure 4G). Taken together, these findings suggest that Rictor deficiency in dermal γδT cells may result in the elevated production of ROS, consequently leading to reduced respiring mitochondria function and IL-17 production.

Because IL-1β-induced mTORC2 activation is through MyD88, we thus examined whether dermal γδT cells from MyD88 KO mice had a similar defect on mitochondrial function and excessive ROS production. Similar to Rictor cKO mice, dermal γδT cells from MyD88 KO mice had decreased respiring mitochondria function (Figure S5A) and increased ROS production as compared with wild-type (WT) mice (Figure S5B). No difference was noticed for glucose uptake as assessed by 2-NBDG binding assay (Figure S5C), consistent with Rictor cKO mice. These data further support the notion that the IL-1β-MyD88-mTORC2 pathway is critical in regulating dermal γδT17 cell function.

IL-23-Mediated STAT3 Signaling Differentially Regulates Vγ4 and Vγ6 Dermal γδT Cell Effector Function

Because IL-23 induces STAT3 activation, we next examined how dermal γδT cell activation is impacted by STAT3 signaling. Skin cells from STAT3 control and cKO mice were stimulated with IL-1β and/or IL-23. The gating strategy was described in Figure S6A. IL-23- or IL-1β-induced dermal γδT cell proliferation was lower in *CD2-cre;STAT3$^{f/f}$* mice (Figure S6B), but IL-17 production was not significantly altered (Figure 5A). It appeared that dermal γδT cells from *CD2-cre;STAT3$^{f/f}$* mice produced even more IL-17 in the presence of both IL-1β and IL-23 (Figure 5A). However, when we gated on the different subsets of dermal γδT cells, we found that dermal Vγ4 T cell proliferation in response to IL-23 stimulation and IL-17 production by IL-1β

(E) Whole skin cell suspensions from CD2-cre;Rictor$^{f/f}$ or control Rictor$^{f/f}$ mice stimulated with IL-23 plus IL-1β at indicated time points and intracellular IL-17 production by dermal γδT cells were assessed by flow cytometry. Flow plots gated on CD3^{+}γδTCR^{int} cells are representative of at least three independent experiments with similar results. Each experiment includes at least two mice from CD2-cre;Rictor$^{f/f}$ or control Rictor$^{f/f}$ strains. Percentages of IL-17-producing γδT cells are shown as mean ± SEM. **p < 0.01, ***p < 0.001 (unpaired Student's t test).

(F) Cultured skin γδT cell lines from CD2-cre;Rictor$^{f/f}$ or control Rictor$^{f/f}$ mice and CD2-cre;Raptor$^{f/f}$ or control Raptor$^{f/f}$ were stimulated with IL-23 for 30 min. p-STAT3 was examined by flow cytometry. Flow histograms gated on CD3^{+}γδTCR^{+} cells are representative of at least three independent experiments with similar results. Each experiment includes at least two mice from CD2-cre;Rictor$^{f/f}$ or control Rictor$^{f/f}$ and CD2-cre;Raptor$^{f/f}$ or control Raptor$^{f/f}$ strains.

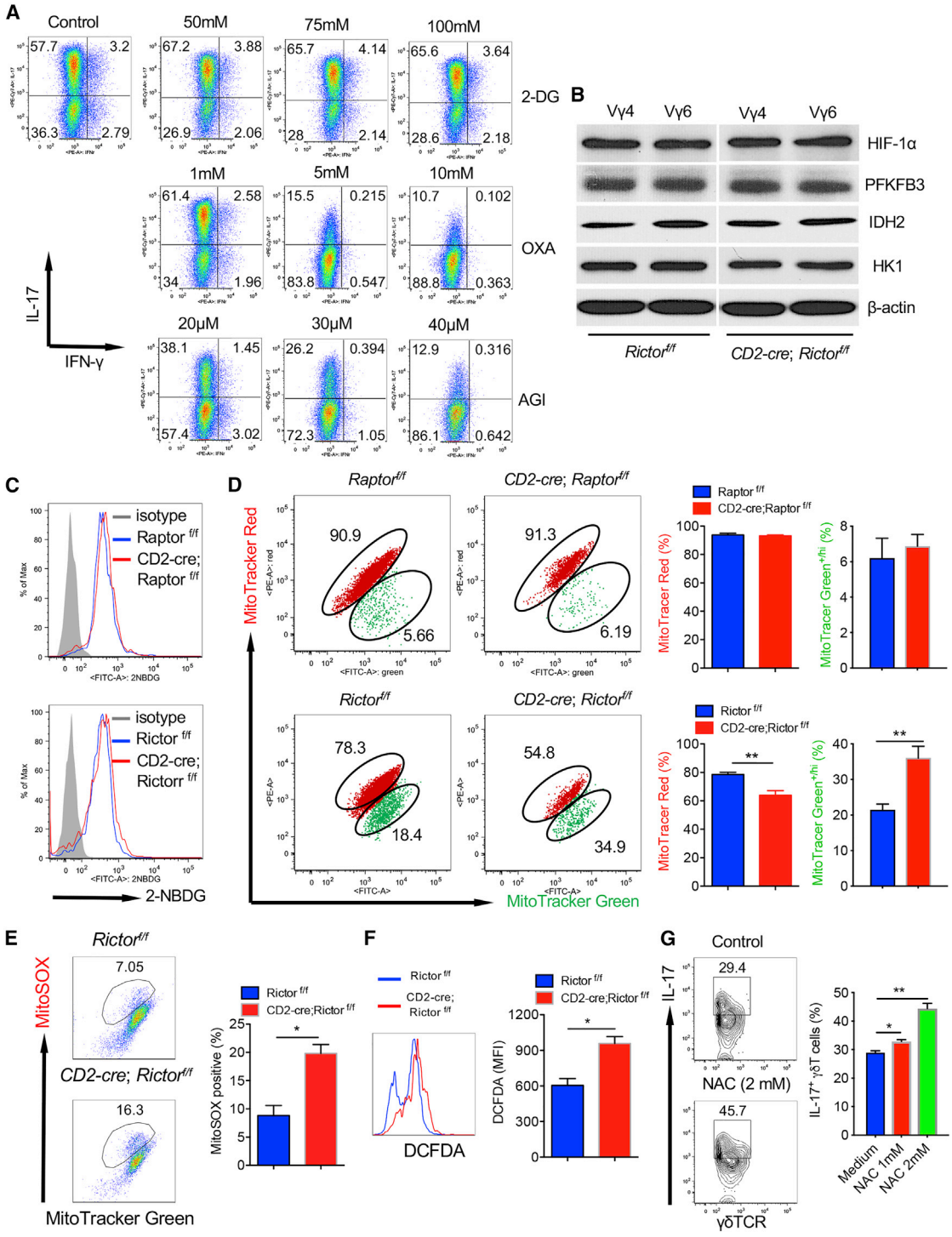

Figure 4. mTORC2 Deficiency in Dermal γδT Cells Leads to Accumulation of Dysfunctional Mitochondria and Production of Mitochondria ROS

(A) γδT cell lines from C57BL/6 WT mice were stimulated with phorbol 12-myristate 13-acetate (PMA)+ionomycin in the presence of varying concentrations of 2-DG, OXA, or AGI for 24 h. Intracellular IL-17 and IFN-γ were examined by flow cytometry. Flow plots gated on $CD3^+\gamma\delta TCR^+$ cells are representative of at least three independent experiments with similar results. Each experiment includes at least three WT mice.

(B) Sorted skin Vγ4 or Vγ6 ($V\gamma4^-$) T cells from cultured γδT cell lines established from CD2-cre;$Rictor^{f/f}$ or control $Rictor^{f/f}$ mice were blotted with indicated molecules including HIF-1α, PFKFB3, IDH2, and HK1.

(legend continued on next page)

and/or IL-23 was drastically reduced in *CD2-cre;STAT3$^{f/f}$* mice (Figure S6C; Figure 5A). In contrast, dermal Vγ6 T cell IL-17 production was somewhat enhanced in *CD2-cre;STAT3$^{f/f}$* mice (Figure 5A), although dermal Vγ6 T cell proliferation was not significantly altered (Figure S6D). We next examined whether mTOR phosphorylation and STAT3 activation in dermal Vγ4 and Vγ6 T cells are different in *CD2-cre;STAT3$^{f/f}$* mice. As shown in Figure 5B, dermal Vγ4 and Vγ6 displayed similar levels of mTOR activation upon IL-1β stimulation. In addition, IL-23-induced STAT3 activation was similarly enhanced in dermal Vγ4 and Vγ6 T cells. These data suggest that STAT3 signal activated by IL-23 differentially regulates effector functions of different subsets of dermal γδT cells.

IL-1R Is Downregulated in STAT3-Deficient Vγ4 T Cells, and IRF-4 Links IL-1R and IL-23R Signaling Pathways for IL-17 Production

Previous data from the Immunological Genome (ImmGen) Project have shown that the IL-17-producing immature Vγ4 T cells (ImmV4e17) and Vγ6 T cells (ImmV6e17) from fetal mice had very similar global gene expression profiles (Narayan et al., 2012). Further analysis showed that 70 genes were differentially expressed on these two subsets (1.5-fold cutoff; Figure 6A). Notably, immV6e17 expressed higher mRNA levels of IL-1R, IL-23R, and IL-7R as compared with immV4e17 (Figure 6B). Indeed, dermal Vγ6 T cells expressed higher levels of IL-1R and IL-23R compared with dermal Vγ4 T cells assessed by flow cytometry (Figure 6C). These data led us to examine whether these receptor expression levels could be regulated differently by STAT3 in dermal Vγ4 and Vγ6 T cells. To this end, we stimulated them with IL-23 or IL-1β+IL-23 and then examined IL-1R and IL-23R expression levels. As shown in Figure 6D, IL-1R mRNA expression level was significantly increased in dermal Vγ4 T cells upon IL-23 stimulation, but not in Vγ6 T cells. Strikingly, the increased IL-1R expression was completely abrogated in dermal Vγ4 T cells from STAT3 cKO mice. However, IL-1R expression on Vγ6 T cells was not altered upon IL-23 stimulation and even was higher in STAT3 cKO mice upon IL-1β and IL-23 stimulation. This was also confirmed by flow cytometry analysis (Figure 6E). In contrast, IL-23R expression was not altered by STAT3 deficiency in both dermal Vγ4 and Vγ6 T cells (data not shown). These findings may explain the differential roles of STAT3 in regulating dermal Vγ4 and Vγ6 effector T cell function.

Next, we examined which transcription factor could link IL-1R and IL-23R signaling pathways for IL-17 production in dermal γδT cells. Transcription factor IRF-4 has been reported previously to play a critical role in Th17 cell differentiation and effector function (Nurieva and Dong, 2008). We found that IRF-4 mRNA expression level was increased upon IL-1β plus IL-23 stimulation in both dermal Vγ4 and Vγ6 T cells, but IL-23 alone did not stimulate elevated IRF-4 expression (Figure 6F). The increased IRF-4 expression was significantly reduced in dermal Vγ4 T cells due to STAT3 deficiency. We also found that IRF-4 mRNA expression was elevated upon IL-1β stimulation, and the elevated IRF-4 expression was abrogated in dermal γδT cells from mTORC2 mice, but not mTORC1 mice (Figure 6G). To further determine the role of IRF-4 in dermal γδ T cells, we used IRF-4 small interfering RNA (siRNA) to knock down IRF-4 expression in dermal γδ T cells. Notably, knockdown of IRF-4 significantly reduced IL-17 production from dermal γδ T cells (Figure 6H).

Skin Inflammation Is Reduced in mTORC2-Deficient Mice, but Not in STAT3-Deficient Mice

Dermal γδT cells play a critical role in skin inflammation. Because mTORC2 has been shown to play an essential role in dermal γδT cell effector function *in vitro*, we examined whether skin inflammation is also impacted by mTORC2 deficiency in mice. In contrast, STAT3 deficiency did not impact on the overall dermal γδT cell effector function, but dermal Vγ4 and Vγ6 T cells were differentially regulated. To this end, we used an imiquimod (IMQ)-induced psoriasis-like mouse model in both strains. Histopathologically, mTORC2-deficient mice had significantly decreased epidermal thickness and neutrophil infiltration as compared with control mice (Figure 7A). The mRNA levels of IL-17 and TNF-α in the skin were also significantly decreased (Figure 7B). In contrast, no significant difference in epidermal thickness and neutrophil infiltration was observed between STAT3 cKO mice (Figure 7C). We also examined *in vivo* 5-bromo-2′-deoxyuridine (BrdU) incorporation to stain proliferating cells in the skin. The gating strategy was shown in Figure S7A. The BrdU incorporation in both dermal Vγ4 and Vγ6 T cells, as well as αβT cells, was significantly decreased in Rictor cKO mice as compared with those in control mice (Figure 7D; Figure S7C). Because dermal γδT cells accounted for more than 95% of IL-17-producing T cells in the skin (Figure S7B), we examined spontaneous IL-17 production from dermal γδT cells. Consistent with *in vitro* observation, total dermal γδT cells

(C) Whole skin cell suspensions from CD2-cre;Rictor$^{f/f}$ or control Rictor$^{f/f}$ mice and CD2-cre;Raptor$^{f/f}$ or control Raptor$^{f/f}$ were stained with 2-NBDG. Expression of 2-NBDG was analyzed by flow cytometry. Flow histograms gated on CD3$^+$γδTCR^{int} cells are representative of at least three independent experiments with similar results. Each experiment includes at least two mice from each strain.

(D) Whole skin cell suspensions from CD2-cre;Rictor$^{f/f}$ or control Rictor$^{f/f}$ mice and CD2-cre;Raptor$^{f/f}$ or control Raptor$^{f/f}$ were stained with MitoTracker Green and MitoTracker Red. Flow plots gated on CD3$^+$γδTCR^{int} cells are representative of at least three independent experiments with similar results. Each experiment includes at least two mice from each strain. Percentages of MitoTracker Green$^{+/hi}$ and MitoTracker Red$^+$ dermal γδT cells are shown as mean ± SEM. **p < 0.01 (unpaired Student's t test).

(E and F) Whole skin cell suspensions from CD2-cre;Rictor$^{f/f}$ or control Rictor$^{f/f}$ mice were stained with MitoSOX for mitochondria ROS production (E) and DCFDA for total ROS production (F). Flow plots (E) or histograms (F) gated on CD3$^+$γδTCR^{int} cells are representative of at least two independent experiments with similar results. Each experiment includes at least two mice from CD2-cre;Rictor$^{f/f}$ or control Rictor$^{f/f}$ strains. Percentage of MitoSOX$^+$ (E) and mean fluorescence intensity (MFI) of DCFDA$^+$ (F) dermal γδ T cells are shown as mean ± SEM. *p < 0.05 (unpaired Student's t test).

(G) Skin γδT cell lines from Rictor cKO mice were stimulated with IL-1β plus IL-23 in the presence of varying concentrations of NAC for 24 h. Intracellular IL-17 was examined by flow cytometry. Flow plots gated on CD3$^+$γδTCR$^+$ cells are combined from two independent experiments with similar results. Data are shown as mean ± SD. *p < 0.05, **p < 0.01 (one-way ANOVA).

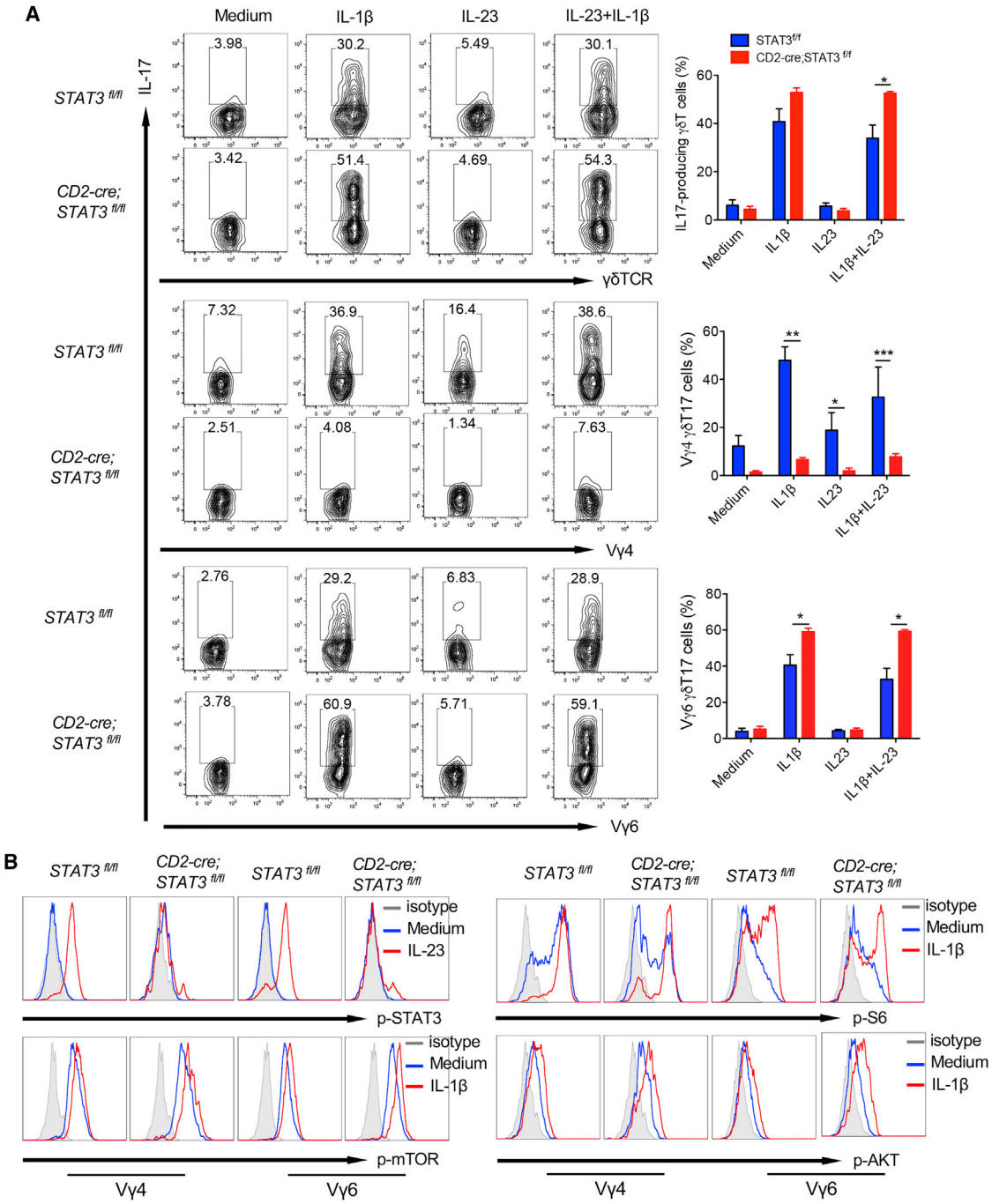

Figure 5. STAT3 Signaling Differentially Regulates Effector Function of Different Subsets of Dermal γδT Cells

(A) Whole skin cell suspensions from CD2-cre;Stat3$^{f/f}$ or control Stat3$^{f/f}$ mice were stimulated with IL-1β, IL-23, or IL-23 plus IL-1β for 48 h. Intracellular IL-17 production by dermal γδT cells was determined by flow cytometry. Flow plots gated on CD3^{+}γδTCR^{int} cells, Vγ4, or Vγ6 T cells are representative of at least three independent experiments with similar results. Each experiment includes at least two mice from CD2-cre;Stat3$^{f/f}$ or control Stat3$^{f/f}$ strains. Percentages of total γδT17, Vγ4T17, and Vγ6T17 cells are shown as mean ± SEM. *p < 0.05, **p < 0.01, ***p < 0.001 (unpaired Student's t test).

(B) Cultured skin γδT cell lines from CD2-cre;Stat3$^{f/f}$ or control Stat3$^{f/f}$ mice were stimulated with IL-23 or IL-1β for 30 min. p-Stat3, p-mTOR, p-AKT, and p-S6 were examined by flow cytometry. Flow histograms gated on CD3^{+}γδTCR^{+}Vγ4 or CD3^{+}γδTCR^{+}Vγ6 cells are representative of at least three independent experiments with similar results. Each experiment includes at least two mice from CD2-cre;Stat3$^{f/f}$ or control Stat3$^{f/f}$ strains.

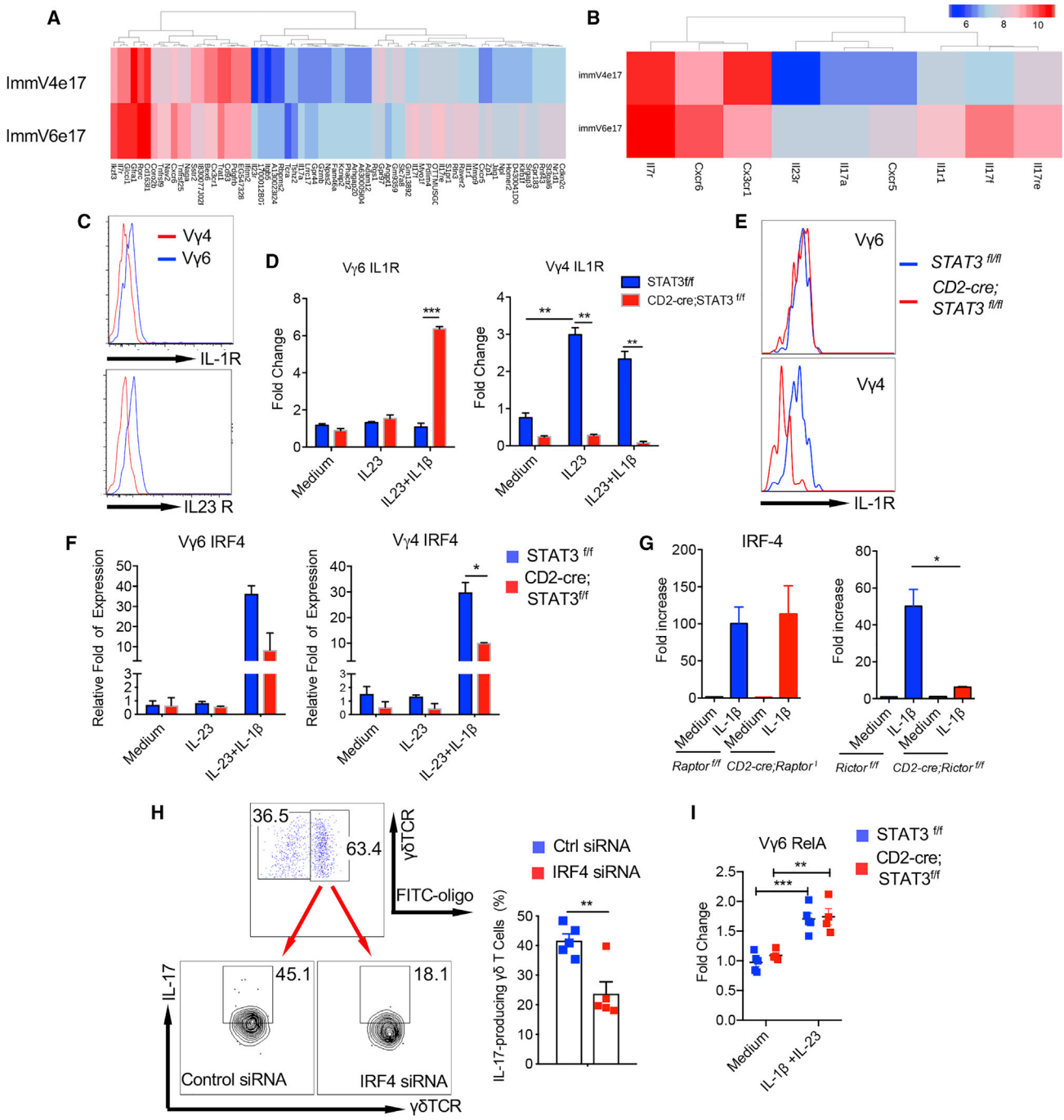

Figure 6. Transcription Factor IRF-4 Links IL-1R and IL-23R Pathways for Enhanced IL-17 Production in Dermal γδT Cells

(A) Differential gene expression in immature fetal Vγ4T17 cells and Vγ6T17 cells (1.5-fold cutoff).

(B) Immature fetal Vγ6T17 cells express higher mRNA levels of *IL-1r*, *IL-23r*, and *IL-7r* than Vγ4T17 cells.

(C) Skin single-cell suspensions were stained for IL-1R and IL-23R on dermal Vγ4 and Vγ6 T cells. Flow plots gated on $CD3^+\gamma\delta TCR^{int}V\gamma4$ or $CD3^+\gamma\delta TCR^{int}V\gamma6$ cells are representative of at least two independent experiments with similar results.

(D) Sorted Vγ4 and Vγ6 T cells from cultured CD2-cre;$Stat3^{f/f}$ or control $Stat3^{f/f}$ skin γδ T cell lines were stimulated with IL-23 or IL-23 plus IL-1β for 3 h. The IL-1R mRNA expression levels were determined by real-time PCR analysis. Summarized data are representative of at least two independent experiments with similar results. Each experiment includes at least two mice from each strain. Data are shown as mean ± SEM. $^{**}p < 0.01$, $^{***}p < 0.001$ (unpaired Student's t test).

(E) IL-1R expression levels on dermal Vγ4 and Vγ6 T cells from CD2-cre;$Stat3^{f/f}$ or control $Stat3^{f/f}$ mice were assessed by flow cytometry. Flow histograms gated on $CD3^+\gamma\delta TCR^{int}$ Vγ4 or $CD3^+\gamma\delta TCR^{int}V\gamma6$ cells are representative of at least three independent experiments with similar results. Each experiment includes at least two mice from CD2-cre;$Stat3^{f/f}$ or control $Stat3^{f/f}$ strains.

(legend continued on next page)

as well as Vγ4 and Vγ6 T cell IL-17 production were significantly reduced in Rictor cKO mice (Figure 7D; Figure S7C). In contrast, BrdU incorporation was significantly reduced in dermal Vγ4, but not Vγ6 or αβT cells, in STAT3 cKO mice (Figure 7E; Figure S7D). Similarly, IL-17 production from total dermal γδT cells was not altered (Figure S7D). However, IL-17 production from dermal Vγ4, but not Vγ6, was significantly reduced in STAT3 cKO mice (Figure 7E). Taken together, these data support the notion that mTORC2 and STAT3 signaling pathways differentially regulate different subsets of dermal γδT effector function *in vivo* leading to distinct outcomes in skin inflammation.

DISCUSSION

Innate stimuli are essential to activate Th17 cells and γδT17 cells. Among these, cytokines including IL-1β and IL-23 have been shown to promote Th17 cell initiation, differentiation, and stabilization (Chang et al., 2013). These cytokines also promote innate γδT cells for enhanced IL-17 production and drive γδT17 cell differentiation and effector function (Muschaweckh et al., 2017; Papotto et al., 2017; Sutton et al., 2009). Although the underlying molecular mechanisms of these cytokines to promote Th17 cell development and function have been well defined (Weaver et al., 2013), how these cytokines induce γδT17 cell effector function remains elusive. The aim of the current study is to investigate the underlying molecular pathways by which dermal γδT17 cells are activated and differentiated. Dermal γδT17 cells have been implicated to be critical in skin inflammatory disease such as psoriasis pathogenesis (Cai et al., 2011; Gray et al., 2011; Harden et al., 2015; Mabuchi et al., 2013; Pantelyushin et al., 2012).

Our study demonstrates that the IL-1β-IL-1R signaling pathway is essential in dermal γδT cell proliferation and IL-17 production. These effects are through the IL-1R-MyD88-mTOR signaling pathway. A previous study shows that the IL-1R-MyD88 pathway is also critical for GM-CSF production by γδT cells (Lukens et al., 2012). IL-1β signaling has been shown to play a critical role during the initial stage of Th17 cell differentiation (Chung et al., 2009). Previous studies have shown that antigen-specific Th17 cells failed to develop in IL1R-deficient mice (Hung et al., 2014). However, γδT17 cells appear to develop normally in the dermis of IL-1R-deficient mice. Similar to Th17 cells, IL-1β also induces phosphorylation of the mTOR in dermal γδT cells. Rapamycin treatment significantly reduces IL-1β-induced dermal γδT cell proliferation and IL-17 production. We show that IL-1β-induced mTOR phosphorylation is completely dependent on adaptor protein MyD88. Notably, mTORC1 and mTORC2 differentially regulate dermal γδT effector function despite the fact that both mTORC1 and mTORC2 pathways are activated in dermal γδT cells upon IL-1β stimulation. We show that IL-1β-induced dermal γδ T cell proliferation and expansion is dependent on both mTORC1 and mTORC2. This is in contrast with a recent study showing enhanced γδT cell generation caused by mTORC1 deficiency (Yang et al., 2018). This discrepancy may be explained by γδT cells from different anatomical sites. Indeed, CD2-cre;Raptor$^{f/f}$ mice have higher γδT cells in the lymph nodes (LNs), but no substantial difference in the skin compared with control mice. However, IL-17 production is mainly dependent on mTORC2, but not mTORC1. It is increasingly recognized that mTOR signaling acts as a central regulator of cellular metabolism in many immune cells (Laplante and Sabatini, 2012). γδT17 cells utilize oxidative phosphorylation as an energy fuel. We show that inhibition of PK and IDH abolishes γδT17 cells. Because mitochondria function is closely related to oxidative phosphorylation, we show that respiring mitochondria is reduced in mTORC2-deficient dermal γδT cells, but not in mTORC1-deficient dermal γδT cells. The decreased respiring mitochondria leads to reduced oxidative phosphorylation, and thus diminished IL-17 production in mTORC2-deficient dermal γδT cells. The reduced respiring mitochondria could be caused by excessive production of nitroxide (NO) because NO is known to inhibit oxidative phosphorylation (Yamasaki et al., 2001). Our data show that ROS production is elevated in the mTORC2-deficient and MyD88 KO dermal γδ T cells, further supporting this notion.

Previous studies have shown that IL-23 signaling is required for Th17 early activation and acquiring pathogenicity (Burkett et al., 2015; Gaffen et al., 2014). IL-23 also drives γδT17 cell differentiation and effector function (Papotto et al., 2017). Here we show that IL-23 synergizes with IL-1β to induce enhanced IL-17 production in dermal γδT cells. This is for both subsets of dermal γδT cells. IL-23 stimulates STAT3 phosphorylation in dermal γδT cells, which is independent of the IL-1R-MyD88-mTOR pathway. However, STAT3 deficiency in dermal γδT cells results in perplexing data by showing decreased γδT cell proliferation and IL-17 production in dermal Vγ4 T cells, but no obvious impact on dermal Vγ6 T cells. A recent study has shown that mouse innate-like αβT cells produce IL-17 independent of STAT3 (St Leger et al., 2018). These innate αβT cells express transcription factor PLZF, whereas Vγ6 T cells also express a high level of PLZF (Lu et al., 2015). Gene expression profiles between Vγ4 and Vγ6 T cells are largely similar, although Vγ6 T cells express

(F) Sorted Vγ4 and Vγ6 T cells from cultured CD2-cre;Stat3$^{f/f}$ or control Stat3$^{f/f}$ skin γδT cell lines were stimulated with IL-23 or IL-23 plus IL-1β for 3 h. The IRF-4 mRNA expression levels were determined by real-time PCR analysis. Summarized data are representative of at least three independent experiments with similar results. Each experiment includes at least three mice from each strain. Data are shown as mean ± SEM. *$p < 0.05$ (unpaired Student's t test).
(G) Sorted γδT cells from cultured CD2-cre;Rictor$^{f/f}$ or control Rictor$^{f/f}$ mice and CD2-cre;Raptor$^{f/f}$ or control Raptor$^{f/f}$ γδ T cells were stimulated with IL-1β for 3 h, and the IRF-4 mRNA expression levels were determined by real-time PCR analysis. Summarized data are representative of at least three independent experiments with similar results. Each experiment includes at least two mice from each strain. Data are shown as mean ± SEM. *$p < 0.05$ (unpaired Student's t test).
(H) Cultured dermal γδT cells from WT mice were transfected with IRF-4 siRNA and/or fluorescein isothiocyanate (FITC)-labeled control siRNA. Cells were then stimulated with IL-1β plus IL-23 for intracellular IL-17 production. Flow plots gated on CD3$^+$γδTCR$^+$ cells are representative of at least three independent experiments with similar results. Percentages of IL-17-producing γδT cells are shown as mean ± SEM. **$p < 0.01$ (unpaired Student's t test).
(I) Sorted Vγ6 T cells from cultured CD2-cre;Stat3$^{f/f}$ or control Stat3$^{f/f}$ skin γδT cell lines were stimulated with IL-23 plus IL-1β for 3 h. The RelA mRNA expression levels were determined by real-time PCR analysis. Summarized data are representative of at least two independent experiments with similar results. Data are shown as mean ± SEM. **$p < 0.01$, ***$p < 0.001$ (unpaired Student's t test).

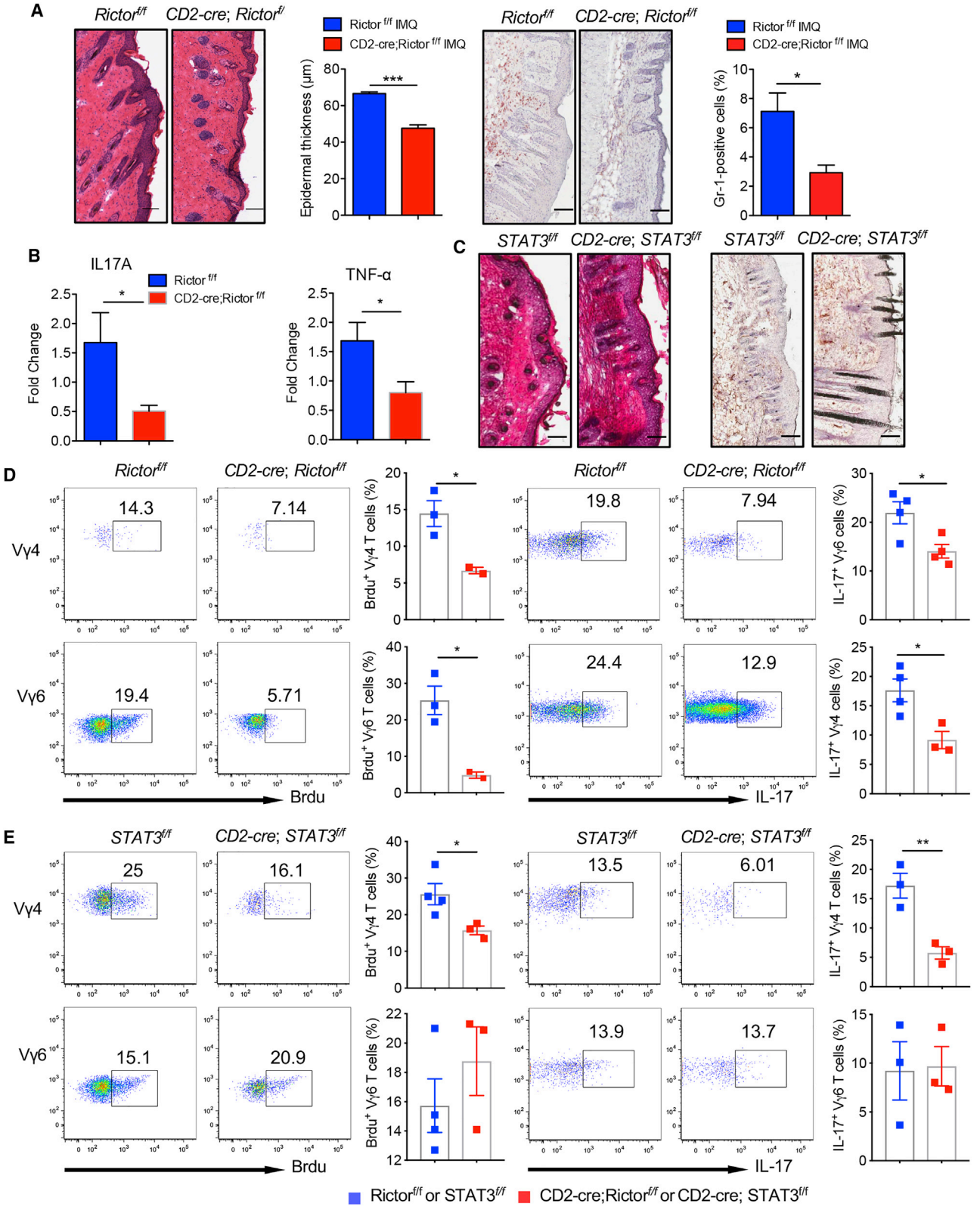

(legend on next page)

higher levels of IL-1R and IL-23R. Notably, IL-1R expression is significantly decreased in STAT3-deficient dermal Vγ4 cells, but not in Vγ6 T cells. This finding may well explain the decreased IL-17 production and proliferation in STAT3-deficient Vγ4 T cells, but not in Vγ6 T cells, upon IL-1β or IL-1β plus IL-23 stimulation. Previous studies have shown that IL-23 induces activation of the STAT3-dependent and STAT3-independent nuclear factor κB (NF-κB) pathway leading to IL-17 production (Cho et al., 2006; Kim et al., 2005). Indeed, dermal Vγ6 T cells have elevated RelA expression upon stimulation, and this is independent of STAT3 activation (Figure 6I). Thus, it is proposed that IL-17 production from dermal Vγ6 T cells may be through the STAT3-independent RelA/NF-κB pathway.

Transcription factor IRF-4 has been shown to bind and govern chromatin accessibility, leading to recruitment of RORγt and binding to Th17 signature genes (Ciofani et al., 2012; Li et al., 2012). We show that IRF-4 expression in dermal γδ T cells is highly stimulated by IL-1β and is abolished in the Rictor cKO mice, but not in Raptor-deficient mice. In addition, IRF-4 expression is also decreased in STAT3-deficient dermal γδ T cells. These data suggest that IRF-4 could be a link between IL-1R and IL-23R signaling pathways for enhanced IL-17 production. This is in contrast with a previous study showing that IRF-4 is not required for γδ T cell IL-17 production (Raifer et al., 2012). However, dermal γδ T cells have unique development pathways that may require differential signaling molecules for their functional activation and differentiation (Cai et al., 2014). Knockdown of IRF-4 in dermal γδ T cells shows reduced IL-17 production, further supporting this notion. Taken together, we propose that dermal γδT cell effector function is regulated through IL-1R and IL-23R pathways. IL-1β activates IRF-4 through the IL-1R-MyD88-mTOC2 pathway for both subsets of dermal γδT cells. In contrast, IL-23 synergizes with IL-1β to induce increased IRF-4 activation in dermal Vγ4 T cells via a STAT3-dependent pathway, whereas dermal Vγ6 T cells may activate IRF-4 via a STAT3-independent RelA pathway leading to IL-17 production. These findings provide critical molecular insight into understanding dermal γδ T cell effector function in skin inflammation.

It has been shown that mTOR signaling plays a critical role in psoriasis pathogenesis (Bürger et al., 2017; Raychaudhuri and Raychaudhuri, 2014). Activation of mTOR signaling in psoriatic skin, particularly in keratinocytes, has been reported previously (Chamcheu et al., 2016). mTOR inhibitors have been tested in the animal models and clinic for the treatment of psoriasis (Bürger et al., 2017; Gao and Si, 2018). Preliminary data suggest that blocking mTOR signaling reduces disease severity (Wei and Lai, 2015). However, it has not been tested whether mTOR deficiency in γδT cells impacts on skin inflammation. We show that IMQ-induced skin inflammation and immunohistopathology are significantly reduced in mTORC2-deficient mice. Consistent with *in vitro* observations, *in vivo* spontaneous IL-17 production and proliferation of dermal γδT cells are significantly decreased in Rictor cKO mice. These findings suggest that mTOR inhibition may primarily impact on dermal γδT cells in the IMQ-induced psoriasis-like mouse model. In addition, our recent data show that IL-1β-induced keratinocyte activation is independent of mTOR signaling, further suggesting that mTOR signaling in dermal γδT cells plays a predominant role in skin inflammation (Cai et al., 2019). Notably, IMQ-induced skin inflammation is abrogated in the MyD88 KO mice (Rabeony et al., 2015), further suggesting critical roles of the IL-1R/MyD88/mTOR signaling pathway in dermal γδT effector function and skin inflammation. In contrast, IL-23-induced STAT3 activation in dermal γδT cells renders no obvious impact on skin inflammation. This is due to differential signaling requirements for dermal Vγ4 versus Vγ6 T cell effector function. We show that dermal Vγ6 T cell proliferation and IL-17 production are independent of STAT3 both *in vitro* and *in vivo*, suggesting that inhibition of STAT3 may not reduce IMQ-induced skin inflammation. It is worth noting that the CD2-cre deletion system also deletes mTORC1 and mTORC2 from αβ T cells. However, dermal γδ T cells are the major IL-17 producer in the skin. It thus proposes that elevated IL-1β in the skin leads to mTOR activation that synergizes with IL-23 to induce dermal γδT cell expansion and enhanced IL-17 production, leading to subsequent skin inflammation.

STAR★METHODS

Detailed methods are provided in the online version of this paper and include the following:

- KEY RESOURCES TABLE
- CONTACT FOR REAGENT AND RESOURCE SHARING
- EXPERIMENTAL MODEL AND SUBJECT DETAILS
  - Mouse models
  - Human subjects
  - Animal procedures

Figure 7. IMQ-Induced Skin Inflammation Is Significantly Reduced in mTORC2-Deficient Mice

(A) CD2-cre;Rictor$^{f/f}$ or control Rictor$^{f/f}$ mice (n = 3) were treated daily for 5 days with IMQ. Representative H&E-stained sections and frozen sections stained with Gr-1 are shown. Gr-1-positive cells are brown. Skin tissues were also stained with CD45 and Gr-1 assessed by flow cytometry. Epidermal thickness at day 5 and percentage of CD45$^+$Gr-1$^+$ cells were measured. Scale bar, 100 μm. Data are representative of three independent experiments with similar results. Data are shown as mean ± SEM. *p < 0.05, ***p < 0.001(unpaired Student's t test).

(B) The mRNA levels of IL-17 and TNF-α from skin tissues were measured by real-time PCR analysis. Data are shown as mean ± SEM. *p < 0.05 (unpaired Student's t test).

(C) CD2-cre;Stat3$^{f/f}$ or control Stat3$^{f/f}$ mice (n = 3–4) were treated daily for 5 days with IMQ. Representative H&E-stained sections and frozen sections stained with Gr-1 are shown. Gr-1-positive cells are brown. Scale bar, 100 μm.

(D and E) CD2-cre;Rictor$^{f/f}$ or control Rictor$^{f/f}$ mice (D) and CD2-cre;Stat3$^{f/f}$ or control Stat3$^{f/f}$ mice (E) were applied topically with IMQ for 5 days. BrdU were injected 1 day before mice were sacrificed. Skin single-cell suspensions were stained for BrdU expression and spontaneous IL-17 production without stimulation. Flow plots gated on CD3$^+$γδTCR^{int}Vγ4 or CD3$^+$γδTCR^{int}Vγ6 cells are representative of two independent experiments with similar results. Percentages of BrdU$^+$Vγ4$^+$ cells and BrdU$^+$Vγ6$^+$ cells and percentages of IL-17-producing Vγ4 and Vγ6 T cells are shown as mean ± SEM. *p < 0.05, **p < 0.01 (unpaired Student's t test).

SUPPLEMENTAL INFORMATION

Supplemental Information can be found online at https://doi.org/10.1016/j.celrep.2019.05.019.

ACKNOWLEDGMENTS

This work was supported by the NIH (R01AI128818), the National Psoriasis Foundation (J.Y.), and the NSFC (81761128008 and 91442123 to J.Z.). X.C. is supported by the China Scholarship Council (CSC 201806230234) and Shanghai Sailing Program (19YF 1427500).

AUTHOR CONTRIBUTIONS

Y.C., F.X., and H.Q. conceived the study; X.C., N.L., and C.F. performed supporting experiments; H.-g.Z., and F.C. provided critical resources; J.Z. supervised the human subject study; and Y.C. and J.Y. provided overall supervision and financial support and wrote the manuscript.

DECLARATION OF INTERESTS

The authors declare no competing interests.

Received: November 20, 2018
Revised: April 4, 2019
Accepted: May 2, 2019
Published: June 4, 2019

REFERENCES

Bürger, C., Shirsath, N., Lang, V., Diehl, S., Kaufmann, R., Weigert, A., Han, Y.Y., Ringel, C., and Wolf, P. (2017). Blocking mTOR Signalling with Rapamycin Ameliorates Imiquimod-induced Psoriasis in Mice. Acta Derm. Venereol. *97*, 1087–1094.

Burkett, P.R., Meyer zu Horste, G., and Kuchroo, V.K. (2015). Pouring fuel on the fire: Th17 cells, the environment, and autoimmunity. J. Clin. Invest. *125*, 2211–2219.

Cai, Y., Shen, X., Ding, C., Qi, C., Li, K., Li, X., Jala, V.R., Zhang, H.G., Wang, T., Zheng, J., and Yan, J. (2011). Pivotal role of dermal IL-17-producing γδ T cells in skin inflammation. Immunity *35*, 596–610.

Cai, Y., Xue, F., Fleming, C., Yang, J., Ding, C., Ma, Y., Liu, M., Zhang, H.G., Zheng, J., Xiong, N., and Yan, J. (2014). Differential developmental requirement and peripheral regulation for dermal Vγ4 and Vγ6T17 cells in health and inflammation. Nat. Commun. *5*, 3986.

Cai, Y., Xue, F., Quan, C., Qu, M., Liu, N., Zhang, Y., Fleming, C., Hu, X., Zhang, H.G., Weichselbaum, R., et al. (2019). A Critical Role of the IL-1β-IL-1R Signaling Pathway in Skin Inflammation and Psoriasis Pathogenesis. J. Invest. Dermatol. *139*, 146–156.

Chamcheu, J.C., Chaves-Rodriquez, M.I., Adhami, V.M., Siddiqui, I.A., Wood, G.S., Longley, B.J., and Mukhtar, H. (2016). Upregulation of PI3K/AKT/mTOR, FABP5 and PPARβ/δ in Human Psoriasis and Imiquimod-induced Murine Psoriasiform Dermatitis Model. Acta Derm. Venereol. *96*, 854–856.

Chang, J., Burkett, P.R., Borges, C.M., Kuchroo, V.K., Turka, L.A., and Chang, C.H. (2013). MyD88 is essential to sustain mTOR activation necessary to promote T helper 17 cell proliferation by linking IL-1 and IL-23 signaling. Proc. Natl. Acad. Sci. USA *110*, 2270–2275.

Cho, M.L., Kang, J.W., Moon, Y.M., Nam, H.J., Jhun, J.Y., Heo, S.B., Jin, H.T., Min, S.Y., Ju, J.H., Park, K.S., et al. (2006). STAT3 and NF-kappaB signal pathway is required for IL-23-mediated IL-17 production in spontaneous arthritis animal model IL-1 receptor antagonist-deficient mice. J. Immunol. *176*, 5652–5661.

Chung, Y., Chang, S.H., Martinez, G.J., Yang, X.O., Nurieva, R., Kang, H.S., Ma, L., Watowich, S.S., Jetten, A.M., Tian, Q., and Dong, C. (2009). Critical regulation of early Th17 cell differentiation by interleukin-1 signaling. Immunity *30*, 576–587.

Ciofani, M., Madar, A., Galan, C., Sellars, M., Mace, K., Pauli, F., Agarwal, A., Huang, W., Parkhurst, C.N., Muratet, M., et al. (2012). A validated regulatory network for Th17 cell specification. Cell *151*, 289–303.

Delgoffe, G.M., Pollizzi, K.N., Waickman, A.T., Heikamp, E., Meyers, D.J., Horton, M.R., Xiao, B., Worley, P.F., and Powell, J.D. (2011). The kinase mTOR regulates the differentiation of helper T cells through the selective activation of signaling by mTORC1 and mTORC2. Nat. Immunol. *12*, 295–303.

Di Meglio, P., Villanova, F., and Nestle, F.O. (2014). Psoriasis. Cold Spring Harb. Perspect. Med. *4*, a015354.

Ding, C., Chen, X., Dascani, P., Hu, X., Bolli, R., Zhang, H.G., Mcleish, K.R., and Yan, J. (2016). STAT3 Signaling in B Cells Is Critical for Germinal Center Maintenance and Contributes to the Pathogenesis of Murine Models of Lupus. J. Immunol. *196*, 4477–4486.

Gaffen, S.L., Jain, R., Garg, A.V., and Cua, D.J. (2014). The IL-23-IL-17 immune axis: from mechanisms to therapeutic testing. Nat. Rev. Immunol. *14*, 585–600.

Gao, M., and Si, X. (2018). Rapamycin ameliorates psoriasis by regulating the expression and methylation levels of tropomyosin via ERK1/2 and mTOR pathways in vitro and in vivo. Exp. Dermatol. *27*, 1112–1119.

Gatzka, M., Hainzl, A., Peters, T., Singh, K., Tasdogan, A., Wlaschek, M., and Scharffetter-Kochanek, K. (2013). Reduction of CD18 promotes expansion of inflammatory γδ T cells collaborating with CD4+ T cells in chronic murine psoriasiform dermatitis. J. Immunol. *191*, 5477–5488.

Gray, E.E., Suzuki, K., and Cyster, J.G. (2011). Cutting edge: Identification of a motile IL-17-producing gammadelta T cell population in the dermis. J. Immunol. *186*, 6091–6095.

Harden, J.L., Hamm, D., Gulati, N., Lowes, M.A., and Krueger, J.G. (2015). Deep Sequencing of the T-cell Receptor Repertoire Demonstrates Polyclonal T-cell Infiltrates in Psoriasis. F1000Res. *4*, 460.

Huang, T., Lin, X., Meng, X., and Lin, M. (2014). Phosphoinositide-3 kinase/protein kinase-B/mammalian target of rapamycin pathway in psoriasis pathogenesis. A potential therapeutic target? Acta. Derm. Venereol. *94*, 371–379.

Hung, C.Y., Jiménez-Alzate, Mdel.P., Gonzalez, A., Wüthrich, M., Klein, B.S., and Cole, G.T. (2014). Interleukin-1 receptor but not Toll-like receptor 2 is essential for MyD88-dependent Th17 immunity to Coccidioides infection. Infect. Immun. *82*, 2106–2114.

Inoki, K., Ouyang, H., Li, Y., and Guan, K.L. (2005). Signaling by target of rapamycin proteins in cell growth control. Microbiol. Mol. Biol. Rev. *69*, 79–100.

Ip, W.K.E., Hoshi, N., Shouval, D.S., Snapper, S., and Medzhitov, R. (2017). Anti-inflammatory effect of IL-10 mediated by metabolic reprogramming of macrophages. Science *356*, 513–519.

Kim, K.W., Cho, M.L., Park, M.K., Yoon, C.H., Park, S.H., Lee, S.H., and Kim, H.Y. (2005). Increased interleukin-17 production via a phosphoinositide 3-kinase/Akt and nuclear factor kappaB-dependent pathway in patients with rheumatoid arthritis. Arthritis Res. Ther. *7*, R139–R148.

Kim, J.S., Sklarz, T., Banks, L.B., Gohil, M., Waickman, A.T., Skuli, N., Krock, B.L., Luo, C.T., Hu, W., Pollizzi, K.N., et al. (2014). Retraction. Nat. Immunol. *15*, 996.

Kulig, P., Musiol, S., Freiberger, S.N., Schreiner, B., Gyülveszi, G., Russo, G., Pantelyushin, S., Kishihara, K., Alessandrini, F., Kündig, T., et al. (2016). IL-12 protects from psoriasiform skin inflammation. Nat. Commun. *7*, 13466.

Kurebayashi, Y., Nagai, S., Ikejiri, A., Ohtani, M., Ichiyama, K., Baba, Y., Yamada, T., Egami, S., Hoshii, T., Hirao, A., et al. (2012). PI3K-Akt-mTORC1-S6K1/2 axis controls Th17 differentiation by regulating Gfi1 expression and nuclear translocation of RORγ. Cell Rep. *1*, 360–373.

Laplante, M., and Sabatini, D.M. (2012). mTOR signaling in growth control and disease. Cell *149*, 274–293.

Lee, K., Gudapati, P., Dragovic, S., Spencer, C., Joyce, S., Killeen, N., Magnuson, M.A., and Boothby, M. (2010). Mammalian target of rapamycin protein complex 2 regulates differentiation of Th1 and Th2 cell subsets via distinct signaling pathways. Immunity *32*, 743–753.

Li, P., Spolski, R., Liao, W., Wang, L., Murphy, T.L., Murphy, K.M., and Leonard, W.J. (2012). BATF-JUN is critical for IRF4-mediated transcription in T cells. Nature *490*, 543–546.

Lowes, M.A., Suárez-Fariñas, M., and Krueger, J.G. (2014). Immunology of psoriasis. Annu. Rev. Immunol. *32*, 227–255.

Lu, Y., Cao, X., Zhang, X., and Kovalovsky, D. (2015). PLZF Controls the Development of Fetal-Derived IL-17+Vγ6+ γδ T Cells. J. Immunol. *195*, 4273–4281.

Lukens, J.R., Barr, M.J., Chaplin, D.D., Chi, H., and Kanneganti, T.D. (2012). Inflammasome-derived IL-1β regulates the production of GM-CSF by CD4(+) T cells and γδ T cells. J. Immunol. *188*, 3107–3115.

Mabuchi, T., Takekoshi, T., and Hwang, S.T. (2011). Epidermal CCR6+ γδ T cells are major producers of IL-22 and IL-17 in a murine model of psoriasiform dermatitis. J. Immunol. *187*, 5026–5031.

Mabuchi, T., Singh, T.P., Takekoshi, T., Jia, G.F., Wu, X., Kao, M.C., Weiss, I., Farber, J.M., and Hwang, S.T. (2013). CCR6 is required for epidermal trafficking of γδ-T cells in an IL-23-induced model of psoriasiform dermatitis. J. Invest. Dermatol. *133*, 164–171.

Martin, B., Hirota, K., Cua, D.J., Stockinger, B., and Veldhoen, M. (2009). Interleukin-17-producing gammadelta T cells selectively expand in response to pathogen products and environmental signals. Immunity *31*, 321–330.

Michel, M.L., Pang, D.J., Haque, S.F., Potocnik, A.J., Pennington, D.J., and Hayday, A.C. (2012). Interleukin 7 (IL-7) selectively promotes mouse and human IL-17-producing γδ cells. Proc. Natl. Acad. Sci. USA *109*, 17549–17554.

Mills, R.E., Taylor, K.R., Podshivalova, K., McKay, D.B., and Jameson, J.M. (2008). Defects in skin gamma delta T cell function contribute to delayed wound repair in rapamycin-treated mice. J. Immunol. *181*, 3974–3983.

Muschaweckh, A., Petermann, F., and Korn, T. (2017). IL-1β and IL-23 Promote Extrathymic Commitment of $CD27^{+}CD122^{-}$ γδ T Cells to γδT17 Cells. J. Immunol. *199*, 2668–2679.

Narayan, K., Sylvia, K.E., Malhotra, N., Yin, C.C., Martens, G., Vallerskog, T., Kornfeld, H., Xiong, N., Cohen, N.R., Brenner, M.B., et al.; Immunological Genome Project Consortium (2012). Intrathymic programming of effector fates in three molecularly distinct γδ T cell subtypes. Nat. Immunol. *13*, 511–518.

Nurieva, R.I., and Dong, C. (2008). Keeping autoimmunity in check: how to control a Th17 cell controller. Immunity *29*, 841–843.

Pantelyushin, S., Haak, S., Ingold, B., Kulig, P., Heppner, F.L., Navarini, A.A., and Becher, B. (2012). Rorγt+ innate lymphocytes and γδ T cells initiate psoriasiform plaque formation in mice. J. Clin. Invest. *122*, 2252–2256.

Papotto, P.H., Gonçalves-Sousa, N., Schmolka, N., Iseppon, A., Mensurado, S., Stockinger, B., Ribot, J.C., and Silva-Santos, B. (2017). IL-23 drives differentiation of peripheral γδ17 T cells from adult bone marrow-derived precursors. EMBO Rep. *18*, 1957–1967.

Rabeony, H., Pohin, M., Vasseur, P., Petit-Paris, I., Jégou, J.F., Favot, L., Frouin, E., Boutet, M.A., Blanchard, F., Togbe, D., et al. (2015). IMQ-induced skin inflammation in mice is dependent on IL-1R1 and MyD88 signaling but independent of the NLRP3 inflammasome. Eur. J. Immunol. *45*, 2847–2857.

Raifer, H., Mahiny, A.J., Bollig, N., Petermann, F., Hellhund, A., Kellner, K., Guralnik, A., Reinhard, K., Bothur, E., Huber, M., et al. (2012). Unlike αβ T cells, γδ T cells, LTi cells and NKT cells do not require IRF4 for the production of IL-17A and IL-22. Eur. J. Immunol. *42*, 3189–3201.

Raychaudhuri, S.K., and Raychaudhuri, S.P. (2014). mTOR Signaling Cascade in Psoriatic Disease: Double Kinase mTOR Inhibitor a Novel Therapeutic Target. Indian J. Dermatol. *59*, 67–70.

Riol-Blanco, L., Ordovas-Montanes, J., Perro, M., Naval, E., Thiriot, A., Alvarez, D., Paust, S., Wood, J.N., and von Andrian, U.H. (2014). Nociceptive sensory neurons drive interleukin-23-mediated psoriasiform skin inflammation. Nature *510*, 157–161.

Sarbassov, D.D., Guertin, D.A., Ali, S.M., and Sabatini, D.M. (2005). Phosphorylation and regulation of Akt/PKB by the rictor-mTOR complex. Science *307*, 1098–1101.

Sarbassov, D.D., Ali, S.M., Sengupta, S., Sheen, J.H., Hsu, P.P., Bagley, A.F., Markhard, A.L., and Sabatini, D.M. (2006). Prolonged rapamycin treatment inhibits mTORC2 assembly and Akt/PKB. Mol. Cell *22*, 159–168.

Sharma, M.D., Rodriguez, P.C., Koehn, B.H., Baban, B., Cui, Y., Guo, G., Shimoda, M., Pacholczyk, R., Shi, H., Lee, E.J., et al. (2018). Activation of p53 in immature myeloid precursor cells controls differentiation into Ly6c+CD103+ monocytic antigen-presenting cells in tumors. Immunity *48*, 91–106.e6.

St Leger, A.J., Hansen, A.M., Karauzum, H., Horai, R., Yu, C.R., Laurence, A., Mayer-Barber, K.D., Silver, P., Villasmil, R., Egwuagu, C., et al. (2018). STAT-3-independent production of IL-17 by mouse innate-like αβ T cells controls ocular infection. J. Exp. Med. *215*, 1079–1090.

Sumaria, N., Roediger, B., Ng, L.G., Qin, J., Pinto, R., Cavanagh, L.L., Shklovskaya, E., Fazekas de St Groth, B., Triccas, J.A., and Weninger, W. (2011). Cutaneous immunosurveillance by self-renewing dermal gammadelta T cells. J. Exp. Med. *208*, 505–518.

Sutton, C.E., Lalor, S.J., Sweeney, C.M., Brereton, C.F., Lavelle, E.C., and Mills, K.H. (2009). Interleukin-1 and IL-23 induce innate IL-17 production from gammadelta T cells, amplifying Th17 responses and autoimmunity. Immunity *31*, 331–341.

Weaver, C.T., Elson, C.O., Fouser, L.A., and Kolls, J.K. (2013). The Th17 pathway and inflammatory diseases of the intestines, lungs, and skin. Annu. Rev. Pathol. *8*, 477–512.

Wei, K.C., and Lai, P.C. (2015). Combination of everolimus and tacrolimus: a potentially effective regimen for recalcitrant psoriasis. Dermatol. Ther. (Heidelb.) *28*, 25–27.

Yamasaki, H., Shimoji, H., Ohshiro, Y., and Sakihama, Y. (2001). Inhibitory effects of nitric oxide on oxidative phosphorylation in plant mitochondria. Nitric Oxide *5*, 261–270.

Yang, K., Blanco, D.B., Chen, X., Dash, P., Neale, G., Rosencrance, C., Easton, J., Chen, W., Cheng, C., Dhungana, Y., et al. (2018). Metabolic signaling directs the reciprocal lineage decisions of αβ and γδ T cells. Sci. Immunol. *3*, eaas9818.

Yoshiki, R., Kabashima, K., Honda, T., Nakamizo, S., Sawada, Y., Sugita, K., Yoshioka, H., Ohmori, S., Malissen, B., Tokura, Y., and Nakamura, M. (2014). IL-23 from Langerhans cells is required for the development of imiquimod-induced psoriasis-like dermatitis by induction of IL-17A-producing γδ T cells. J. Invest. Dermatol. *134*, 1912–1921.

Zeng, H., and Chi, H. (2013). mTOR and lymphocyte metabolism. Curr. Opin. Immunol. *25*, 347–355.

Zeng, X., Wei, Y.L., Huang, J., Newell, E.W., Yu, H., Kidd, B.A., Kuhns, M.S., Waters, R.W., Davis, M.M., Weaver, C.T., and Chien, Y.H. (2012). γδ T cells recognize a microbial encoded B cell antigen to initiate a rapid antigen-specific interleukin-17 response. Immunity *37*, 524–534.

Zeng, H., Yang, K., Cloer, C., Neale, G., Vogel, P., and Chi, H. (2013). mTORC1 couples immune signals and metabolic programming to establish T(reg)-cell function. Nature *499*, 485–490.

Zuberbuehler, M.K., Parker, M.E., Wheaton, J.D., Espinosa, J.R., Salzler, H.R., Park, E., and Ciofani, M. (2019). The transcription factor c-Maf is essential for the commitment of IL-17-producing γδ T cells. Nat. Immunol. *20*, 73–85.

STAR★METHODS

KEY RESOURCES TABLE

REAGENT or RESOURCE	SOURCE	IDENTIFIER
Antibodies		
anti-mouse CD3 clone 17A2, PerCP-Cy5	BioLegend	Cat# 100218; RRID: AB_1595492
anti-mouse TCR$\gamma\delta$ clone GL3, APC	BioLegend	Cat# 118116; RRID: AB_1731813
anti-mouse Vγ4 clone UC3-10A6, PE	BioLegend	Cat# 137706; RRID: AB_10643577
anti-mouse Vγ4 clone UC3-10A6, FITC	BioLegend	Cat# 137704; RRID: AB_10569353
anti-mouse Vγ6 clone 17D1	Dr. Tigelaar (Department of Dermatology, Yale university)	N/A
anti-mouse CD45 clone 30-F11, FITC	BioLegend	Cat# 103108; RRID: AB_312973
anti-mouse CD4 clone GK1.5, PE	BioLegend	Cat# 100408; RRID: AB_312693
anti-mouse CD8 clone 53-6.7, PE	BioLegend	Cat# 100708; RRID: AB_312747
anti-mouse Gr-1 clone RB6-8C5, PE	BioLegend	Cat# 108408; RRID: AB_313373
anti-mouse IL-17A clone TC11-18H10.1, PE-Cy7	BioLegend	Cat# 506922; RRID: AB_2125010
anti-mouse Brdu clone 3D4, FITC	BioLegend	Cat# 364104; RRID: AB_2564481
anti-rabbit IgG (minimal x-reactivity) clone Poly4064, FITC	BioLegend	Cat# 406403; RRID: AB_893531
anti-rabbit IgG (minimal x-reactivity) clone Poly4064, PE	BioLegend	Cat# 406421; RRID: AB_2563484
anti-mouse CD3 clone 17A2, purified	BioLegend	Cat# 100208; RRID: AB_312665
anti-mouse phospho Stat3 (Tyr705) clone D3A7	Cell Signaling Technology	Cat# 9145; RRID: AB_2491009
anti-mouse phospho AKT (Ser473) clone 193H12	Cell Signaling Technology	Cat# 4058; RRID: AB_331168
anti-mouse phospho S6 Ribosomal protein (Ser235/236) clone D57.2.2E	Cell Signaling Technology	Cat# 4858; RRID: AB_916156
anti-mouse mTOR (phospho Ser2448) [EPR426 (2)]	Abcam	Cat# ab109268; RRID: AB_10888105
anti-mouse phospho mTOR (Ser2448)	Cell Signaling Technology	Cat# 2971; RRID: AB_330970
DCFDA / H2DCFDA - Cellular ROS Assay Kit	Abcam	Cat# ab113851
MitoTracker Green	Thermo Fisher SCIENTIFIC	Cat# M7514
MitoTracker Red	Thermo Fisher SCIENTIFIC	Cat# M7512
MitoSOX	Thermo Fisher SCIENTIFIC	Cat# M36008
anti-mouse Gr-1, purified	Homemade	N/A
anti-Rabbit IgG, HRP	GE Healthcare life sciences	Cat# NA934
anti-Rat IgG, HRP	Santa Cruz	Cat# sc-2006
Biological Samples		
Skin tissues from patients with psoriasis vulgaris	Department of Dermatology, Ruijin Hospital, Shanghai Jiaotong University School of Medicine	N/A
Chemicals, Peptides, and Recombinant Proteins		
Aldara (5% Imiquimod)	3M Pharmaceuticals	N/A
Dulbecco's Phosphate Buffered Saline (PBS)	Millipore Sigma	Cat# D8537
RPMI 1640	Millipore Sigma	Cat# R8758
Phorbol 12-myristate 13-acetate (PMA)	Millipore Sigma	Cat# P8139
Ionomycin calcium salt from Streptomyces conglobatus	Millipore Sigma	Cat# I0634
5-Bromo-2′-deoxyuridine (Brdu)	Millipore Sigma	Cat# B5002
AEC Peroxidase (HRP) Substrate Kit	VECTOR LABORATORIES	Cat# SK-4200; RRID: AB_2336076
Collagenase	Millipore Sigma	Cat# C9891
Hyaluronidase	Millipore Sigma	Cat# H2126
Deoxyribonuclease (DNase) I	Millipore Sigma	Cat# D5025
Recombinant mouse IL-7 (carrier-free)	BioLegend	Cat# 577806

(*Continued on next page*)

Continued

REAGENT or RESOURCE	SOURCE	IDENTIFIER
Recombinant mouse IL-23 (carrier-free)	BioLegend	Cat# 589006
Recombinant mouse IL-1β (carrier-free)	BioLegend	Cat# 575106
CellTrace™ CFSE Cell Proliferation Kit, for flow cytometry	Thermo Fisher SCIENTIFIC	Cat# C34554
AGI-5198	Millipore Sigma	Cat# SML0839
Sodium oxalate	Millipore Sigma	Cat# O0136
2-Deoxy-D-glucose (2-DG)	Millipore Sigma	Cat# D8375
N-acetylcysteine	Millipore Sigma	Cat# A7250
7-AAD Viability Staining Solution	BioLegend	Cat# 420404
eBioscience™ Fixable Viability Dye eFluor™ 780	Thermo Fisher SCIENTIFIC	Cat# 65-0865-14
Brefeldin A Solution (1,000X)	BioLegend	Cat# 420601
Fixation Buffer	BioLegend	Cat# 420801
Intracellular Staining Permeabilization Wash Buffer (10X)	BioLegend	Cat# 421002
DAPI (4', 6-Diamidino-2-Phenylindole, Dihydrochloride)	Thermo Fisher SCIENTIFIC	Cat# D1306
TRIzol Reagent	Thermo Fisher SCIENTIFIC	Cat# 15596018
RNeasy Mini Kit	QIAGEN	Cat# 74104
iScript cDNA Synthesis Kit	Bio-Rad	Cat# 170-8891
iQ SYBR® Green Supermix	Bio-Rad	Cat# 1708882
Deposited Data		
RNaseq	This paper	GSE114729
Experimental Models: Organisms/Strains		
C57BL/6J	The Jackson Laboratory	Stock# 000664; RRID: IMSR_JAX:000664
MyD88−/−	The Jackson Laboratory	Stock# 009088; RRID: IMSR_JAX:009088
IL-1R−/−	The Jackson Laboratory	Stock# 003245; RRID: IMSR_JAX:003245
hCD2-Cre	The Jackson Laboratory	Stock# 008520; RRID: IMSR_JAX:008520
$Raptor^{fl/fl}$	The Jackson Laboratory	Stock# 013188; RRID: IMSR_JAX:013188
$Rictor^{fl/fl}$	The Jackson Laboratory	Stock# 020649; RRID: IMSR_JAX:020649
$Stat3^{fl/fl}$	Dr. Shizuo Akira	N/A
Oligonucleotides		
FITC-conjugated control siRNA	Santa Cruz Biotechnology	Cat# sc-36869
IRF4 siRNA	Santa Cruz Biotechnology	Cat# sc-35713
Primers IL-17A murine	QIAGEN	Cat# QT00103278
TNF-α (murine): Forward: TGTAGCCCACGTCGTAGCAAA	This paper	N/A
TNF-α (murine): Reverse: CTGGCACCACTAGTTGGTTGT	This paper	N/A
IL-1R (murine): Forward: CGCAGAAGCTGAAGTCTACG	This paper	N/A
IL-1R (murine): Reverse: CAGGTGGCAGAAAGTCTAGA	This paper	N/A
IRF4 (murine): Forward: CCATTGAGCCAAGCATAAGG	This paper	N/A
IRF4 (murine): Reverse: CTCGTCGTGGTCAGCTCTTT	This paper	N/A
RelA (murine): Forward: GTATTGCTGTGCCTACCCGA	This paper	N/A
RelA (murine): Reverse: CATGGGGGAAAACTCATCAA	This paper	N/A
Software and Algorithms		
FlowJo	FlowJo, LLC	https://www.flowjo.com
GraphPad Prism	N/A	https://www.graphpad.com
Aperio ImageScope	Leica BIOSYSTEMS	https://www.leicabiosystems.com/digital-pathology/scan/

CONTACT FOR REAGENT AND RESOURCE SHARING

Further information and requests for resources and reagents should be directed to and will be fulfilled by the Lead Contact, Jun Yan (jun.yan@louisville.edu).

EXPERIMENTAL MODEL AND SUBJECT DETAILS

Mouse models

C57BL/6 WT, MyD88$^{-/-}$ and *Il1r1*$^{-/-}$ mice on C57BL/6 background were purchased from the Jackson Laboratory. IL-23R KO mice were imported from Genetech. hCD2-Cre mice (Jackson Laboratory) were crossed with Raptor$^{fl/fl}$ mice, Rictor$^{fl/fl}$ mice (Jackson Laboratory) and Stat3$^{fl/fl}$ mice (Ding et al., 2016) to generate CD2-cre;Raptor$^{fl/fl}$, CD2-cre;Rictor$^{fl/fl}$ and CD2-cre;Stat3$^{fl/fl}$ conditional KO (cKO) mice. Male and female mice were used in all experiments (6-12 weeks old) and were housed in specific pathogen free conditions. All experiments were in accordance with institutional guidelines and approved by the IACUC at the University of Louisville.

Human subjects

Patients with psoriasis vulgaris were diagnosed based on the clinical and histopathologic criteria. For RNaseq study, total 21 patients (age, 27-69; female 4, male 17) with psoriasis vulgaris were enrolled. All patients had not been treated systemically for at least 4 weeks or topical treatment for at least 2 weeks prior to the study entry. Patients were treated with topical halomethasone monohydrate 0.05% cream daily for 2 weeks. Skin lesion severity was evaluated by PASI (psoriasis area and severity index) score. A 50% reduction in the PASI score was considered as effective treatment. Typical lesions that represented the overall skin condition before and after treatment were taken. RNAs were extracted and library was made and sequenced with sequencing platform BGISEQ-500 (BGI). The sample sequences were directly aligned to the *Homo sapiens* reference genome assembly using tophat2 (version 2.0.13), generating alignment files. The number of reads is between 37 to 52 million. RNA-Seq data have been deposited into NCBI GEO with the accession number (GSE114729). All participants were recruited from Department of Dermatology, Ruijin Hospital, Shanghai Jiaotong University School of Medicine. These studies were approved by the Shanghai Jiaotong University School of Medicine Research Ethics Committee. All the participants gave their written informed consent.

Animal procedures

Establishment of psoriasis-like mouse models

Imiquimod (IMQ)-induced psoriasis-like mouse model was established as previously described (Cai et al., 2014). Briefly, CD2-cre;Rictor$^{f/f}$ and control Rictor$^{f/f}$ mice or CD2-cre;Stat3$^{f/f}$ and control Stat3$^{f/f}$ mice were applied daily with IMQ cream (5%) (Aldara; 3M Pharmaceuticals) on the shaved back for 5 consecutive days. Mice were sacrificed on day 5. The skin samples were embedded and frozen in OCT for H&E and immunohistochemistry (IHC) staining. Additionally, skin samples were excised in TRIzol (Thermo Fisher SCIENTIFIC) for RNA extraction. Skin cell suspensions from IMQ-treated skin were also stained for CD45, Gr-1, CD3, γδTCR and intracellular IL-17 and percentages of CD45^{+}Gr-1^{+} cells as well as IL-17 production were determined by flow cytometry.

BrdU in vivo incorporation assay

CD2-cre;Rictor$^{f/f}$ and control Rictor$^{f/f}$ mice or CD2-cre;Stat3$^{f/f}$ and control Stat3$^{f/f}$ mice were applied daily with IMQ cream (5%) (Aldara; 3M Pharmaceuticals) on the shaved back for 5 consecutive days. Mice was intraperitoneally injected BrdU (2 mg/mouse, Millipore Sigma) on day 5. After 24 hours, mouse skin cells from IMQ-treated skin were stained with anti-BrdU antibody (Ab) (clone 3D4, Biolegend) and Brdu^{+} cells were determined by flow cytometry.

Skin histology and immunohistochemical (IHC) staining

Skin sections from IMQ-treated skin were embedded and frozen in OCT and stained with H&E and Gr-1 mAb for IHC. Epidermal thickness was determined by measuring the average interfollicular distance under the microscope in a blinded manner. For IHC staining, skin cryosections were fixed, blocked and then stained with purified rat-anti-mouse Gr-1 Ab (1:50 dilution) following with goat-anti-rat IgG secondary antibody (1:200 dilution, Southern Biotech). Slides were developed with AEC substrate solution (Vector Laboratories) and then counterstained with hematoxylin. Images were acquired at x200 magnification using Aperio ScanScope digital scanners.

METHOD DETAILS

Tissue processing, cell culture and stimulation

Tissue preparation

Whole skin cells from mouse back skin were prepared as previously described (Cai et al., 2011). Briefly, mouse back skin was cut into small pieces and digested with a buffer containing collagenase IV (Millipore Sigma), hyaluronidase (Millipore Sigma), and DNase-I (Millipore Sigma) at 37°C for 2 hours. The tissue was further homogenized with a syringe and filtered through a 40 μm cell strainer. Whole skin single cell suspensions were obtained by centrifugation. Single cell suspensions from peripheral lymph nodes were prepared by mashing the lymph nodes through 40 μm cell strainers.

Establishment of skin γδ T cell line

Mouse skin γδ T cell line was generated *in vitro* from whole skin cell suspensions. Briefly, whole skin cell suspensions were prepared as described above. At day 3, purified anti-mouse CD3 antibody (0.1 μg/ml, Biolegend) were added into the culture followed by adding recombinant mouse IL-7 (rmIL-7) (5 ng/ml, Biolegend) on the next day and day 7. Cells were expanded and cultured for total 10-14 days. The percentage of dermal γδ T cells was determined by flow cytometry.

Cell sorting

Mouse skin γδ T cell lines were established as described above and stained with anti-mouse CD3, γδ TCR and/or Vγ4 Abs. Skin γδ T cells or skin $V\gamma4^+$ or $V\gamma4^-$ T cells were sorted by MoFlow high-speed sorter or BD FACSAria III cell sorter for western blot analysis or real-time PCR.

Cell stimulation

Whole skin cell suspensions were stimulated with rmIL-23 (5ng/ml, Biolegend), rmIL-1β (10ng/ml, Biolegend), or rmIL-23 plus rmIL-1β for indicated times. Intracellular IL-17 was measured by flow cytometry. In proliferation assay, whole skin cells were labeled with CFSE (1 μM, Thermo Fisher SCIENTIFIC) and then stimulated with rmIL-23, rmIL-1β, or rmIL-23 plus rmIL-1β for 3 days. Cell proliferation and intracellular IL-17 were measured by flow cytometry. For Rapamycin inhibition assay, whole skin cell suspensions were stimulated with mouse rmIL-23 plus rmIL-1β for 3 days in the absence or presence of Rapamycin (Millipore Sigma). In metabolic inhibition experiments, AGI-5198 (Millipore Sigma), sodium oxalate (Millipore Sigma), and 2-DG (Millipore Sigma) were added in the culture at indicated concentrations. For NAC assay, skin γδ T cell lines were stimulated with rmIL-1β and rmIL-23 in the varying concentrations of NAC for 24 h and intracellular IL-17 was determined by flow cytometry. In addition, whole skin cells or lymphocytes were also stimulated with PMA plus ionomycin for 5 hours in the presence of Golgi-Plug. Whole skin cells from IMQ-treated skin were incubated with Golgi-Plug only at 37°C for 5 hours. Intracellular IL-17 level was determined by flow cytometry. In dermal γδ T cell signaling studies, mouse skin γδ T cell line or sorted skin $V\gamma4^+$ or $V\gamma4^-$ from skin γδ T cell line was stimulated with rmIL- 23, rmIL-1β, or rmIL-23 plus rmIL-1β for indicated times. Phosphorylation of indicated molecules was measured by flow cytometry or western blot analysis. mRNA levels of transcriptional factor IRF4 and IL-1R were also determined by real-time quantitative PCR (qPCR) analysis.

IRF4 siRNA transfection

Primary skin γδ T cell lines were seeded into 24-well plates with RPMI-1640 containing 20% FBS and mIL-7 (3ng/ml, Biolegend) for overnight culture. FITC-conjugated control siRNA (sc-36869, Santa Cruz Biotechnology) or IRF4 siRNA (sc-35713, Santa Cruz Biotechnology) was added into the culture with lipofetcamine^{TM}2000 reagent (11668-027, Thermo Fisher SCIENTIFIC). A small amount of FITC-conjugated siRNA was added into the IRF4 siRNA transfection well. After 5 hours incubation, fresh RPMI-1640 medium containing 3 ng/ml mIL-7 was added and cells were continued to culture for additional 24 hours. Cells were then stimulated with mIL-1β (10ng/ml) and mIL-23 (10ng/ml) for 48 hours and intracellular IL-17 staining was performed. Transfected cells positive for FITC-conjugated siRNA were gated for flow analysis as described previously (Sharma et al., 2018).

Flow cytometry

All utilized Abs are summarized in the Key Resources Table. Samples were harvested with BD FACS Canton (Becton Dickinson, San Jose, CA, USA) and analyzed with FlowJo software (TreeStar).

Surface staining and intracellular staining

For surface staining, cells were first blocked with anti-CD16/32 (clone 2.4G2) and then stained with different cell surface Abs at 4°C for 20min. The relevant isotype control mAbs were also used. For intracellular cytokine staining, cells were stained with surface Abs first. Then cells were fixed and permeabilized (Biolegend) followed by intracellular staining for IL-17 at 4°C for 45min.

Phospho flow staining

For phospho-Stat3 (p-Stat3), p-AKT and p-S6 Ribosomal protein flow staining, mouse skin cells were fixed in 4% paraformaldehyde and then permeabilized in 90% cold methanol. Cells were stained with rabbit-anti-mouse p-Stat3 (Tyr705), p-AKT (Ser473) or p-S6 Ribosomal protein (Ser235/236) (Cell Signaling Technology) at 4°C overnight. For phospho-mTOR staining, cells were fixed in 4% paraformaldehyde and then permeabilized in Tween-20. Cells were stained with rabbit-anti-mouse p- mTOR (Ser2448, Abcam) at 4°C overnight. On next day, cells were washed and stained with fluorochrome-labeled donkey anti-rabbit IgG Ab, anti-mouse CD3, γδ TCR and Vγ4 at room temperature for 30min.

Measurement of mitochondrial content

For MitoTracker Green and MitoTracker Red staining, fresh mouse skin cells or stimulated skin cells were suspended in prewarmed PBS with 0.1% BSA. Cells were first blocked with anti-CD16/32 and then stained with MitoTracker Green (Thermo Fisher SCIENTIFIC, 80nM) and MitoTracker Red (Thermo Fisher SCIENTIFIC, 20nM) at 37°C for 30min. Cells were then stained with different cell surface Abs at 4°C for 20 min. For MitoSOX staining, fresh mouse skin cells or stimulated skin cells were suspended in prewarmed PBS with 0.1%BSA. Cells were stained with MitoTracker Green (80nM) and incubated at 37°C for 30 min. Cells were washed with prewarmed HBSS including Ca^{2+} and Mg^{2+} and stained with MitoSOX (Thermo Fisher SCIENTIFIC, 5 μM) at 37°C for 15min. Cells were then stained with different cell surface Abs at 4°C for 20 min. For DCFDA-Cellular Reactive Oxygen Species (ROS) staining, cells were first blocked with anti-CD16/32 and then stained with DCFDA (Abcam, 20 μM) at 37°C for 30min. Cells were washed and stained with different cell surface Abs at 4°C for 20 min.

Brdu staining

Mouse skin cells from IMQ-treated skin were stained with viability dye, anti-mouse CD3, γδ TCR, Vγ4, Vγ6 and CD45. After fixation and treatment with DNase I (Millipore Sigma), cells were stained with anti-mouse BrdU Ab (clone 3D4, Biolegend) and then measured by flow cytometry.

Immunofluorescence (IF) staining

Sorted mouse $CD45^+CD4^-CD8^-$ cells from C57BL/6 WT cultured skin γδ T cell lines were stimulated with rmIL-23 (5ng/ml) or rmIL-1β (10ng/ml) at 37°C for 30min. Cells were fixed with 4% paraformaldehyde and then permeabilized with 0.3% (v/v) Triton X-100. Cells were incubated with anti-γδTCR (Biolegend) and anti-p-Stat3 (Tyr705, Cell Signaling Technology) or anti-p-mTOR (Ser2448, Abcam) at 4 °C overnight followed by donkey anti-rabbit secondary Ab and DAPI for nucleus. Images were acquired with fluorescence microscope (Nikon).

Western blot analysis

For immunoblot analysis, mouse skin γδ T cells or skin $V\gamma4^+$ and $V\gamma4^-$ T cells were sorted from cultured skin γδ T cell line and stimulated with rmIL-1β, rmIL-23, rmIL-1β plus rmIL-23 for indicated times. Cells were lysed in Triton X-100 lysis buffer containing protease and phosphatase inhibitors. The whole-cell extracts were separated by SDS-PAGE and electrotransferred to a polyvinylidene difluoride membrane. After blocking, the membranes were probed overnight at 4°C with appropriate primary Abs and then secondary Ab. The primary Abs included p-Stat3 (Tyr705), p-AKT (Ser473), p-S6 Ribosomal protein (Ser235/236), and p-mTOR (Ser2448) (Cell Signaling Technology). The blots were developed using ECL Plus western blotting Detection Reagents (GE Healthcare).

RNA extraction and real-time quantitative PCR (qPCR)

RNAs were isolated using a QIAGEN RNeasy kit according to the manufacturer's instructions (QIAGEN) or TRIzol (Thermo Fisher SCIENTIFIC). After reverse transcription into cDNA with a Reverse Transcription Kit (Bio-Rad), qPCR was then performed on Bio-Rad CFX Connect™ Real-time system (Bio-Rad) using SYBR Green (Bio-Rad) and gene-specific primers were listed as follows: mouse IL-17A (Mm_Il17a_SG, QIAGEN) were purchased from QIAGEN; other primers were described in the Key Resources Table. Mouse gene expression level was normalized to mouse β-2 microglobulin (β-MG) housekeeping gene and represented data as fold differences by the $2^{-\Delta\Delta Ct}$ method, where ΔCt = Ct(target gene)-Ct(β-MG) and ΔΔCt = ΔCt(induced)-ΔCt(reference).

QUANTIFICATION AND STATISTICAL ANALYSIS

Statistical analysis

All quantitative data are shown as mean ± s.e.m unless otherwise indicated. All samples were compared using two-tailed, unpaired Student's T test or one-way ANOVA if more than two groups were compared. A *P value* less than 0.05 was considered significant. Statistical analysis was performed with GraphPad Prism software.

Cell Reports, Volume *27*

Supplemental Information

Differential Roles of the mTOR-STAT3 Signaling in Dermal γδ T Cell Effector Function in Skin Inflammation

Yihua Cai, Feng Xue, Hui Qin, Xu Chen, Na Liu, Chris Fleming, Xiaoling Hu, Huang-ge Zhang, Fuxiang Chen, Jie Zheng, and Jun Yan

Supplementary Figures

Figure S1

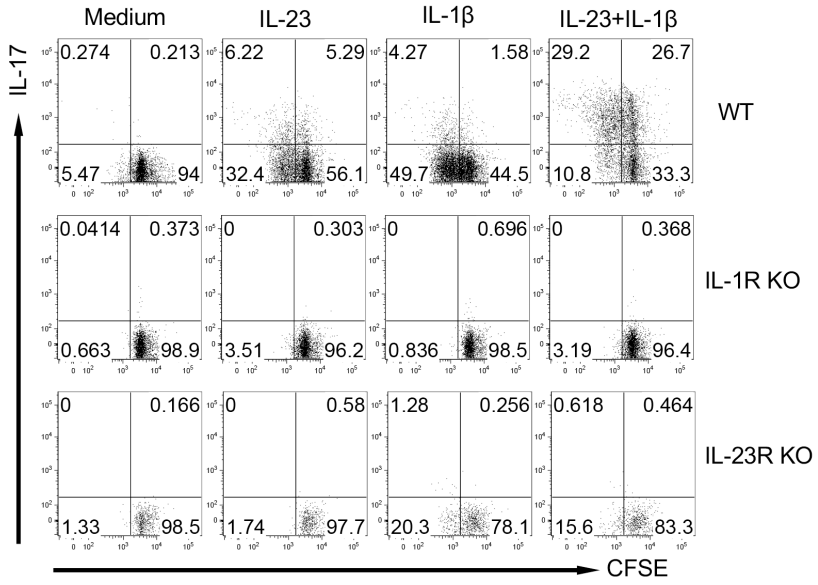

Figure S1. IL-1R and IL-23R signaling pathways regulate dermal γδT cell expansion and IL-17 production. Whole skin cell suspensions from WT, IL-1R KO and IL-23R KO mice were labeled with CSFE and then stimulated with IL-23, IL-1β, or IL-23 plus IL-1β for 3 days. Cell proliferation and intracellular IL-17 were analyzed by flow cytometry. Flow plots gated on $CD3^{+}\gamma\delta TCR^{int}$ cells are representative of at least two independent experiments with similar results. Each experiment includes at least three mice from WT, IL-1R KO or IL-23R KO strains. Related to Figure 1.

Figure S2

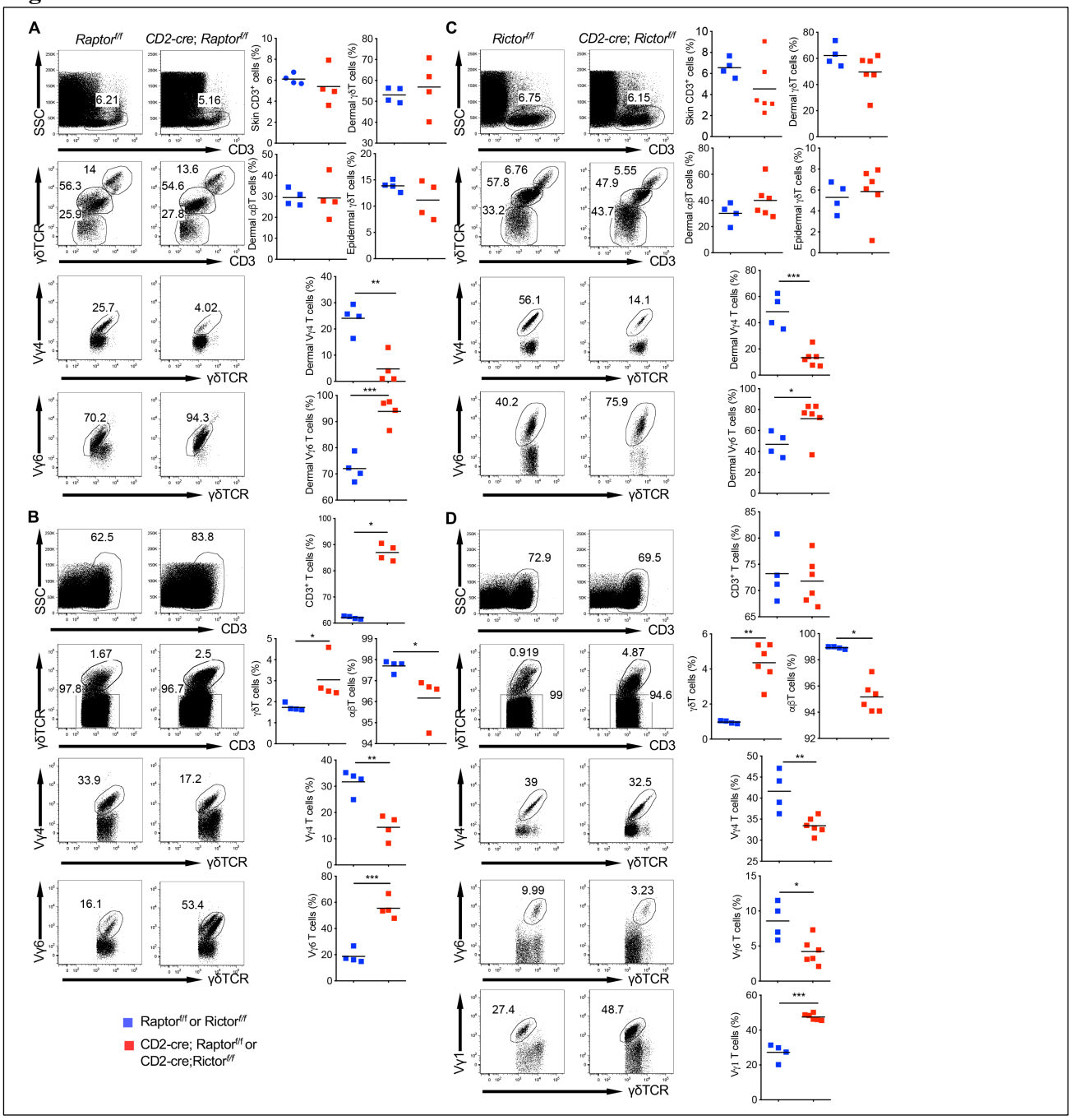

Figure S2. mTOR signaling is critical in γδT cell homeostasis in the periphery. (A, B) Skin tissues (A) and lymph nodes (B) from control Raptor$^{f/f}$ mice and CD2-cre;Raptor$^{f/f}$ mice were stained with CD3, αβTCR, γδTCR, Vγ4, and Vγ6. Percentages of CD3+ T cells, αβT cells, dermal γδT cells (CD3^{+}γδTCR^{int}) and epidermal γδT cells (CD3^{+}γδTCR^{hi}) and different subsets of γδT cells are shown. Data are are representative of at least two independent experiments with similar results. Data are shown as mean ± SEM. *p<0.05, **p<0.01, ***p<0.001 (unpaired Student's t test). (C, D) Skin tissues (C) and lymph nodes (D) from control Rictor$^{f/f}$ mice and CD2-cre;Rictor$^{f/f}$ mice were stained with CD3, αβTCR, γδTCR, Vγ4, and Vγ6. Percentages of CD3+ T cells, αβT cells, dermal γδT cells (CD3^{+}γδTCR^{int}) and epidermal γδT cells (CD3^{+}γδTCR^{hi}) and different subsets of γδT cells are shown. Data are are representative of at least two independent experiments with similar results. Data are shown as mean ± SEM. *p<0.05, **p<0.01, ***p<0.001 (unpaired Student's t test). Related to Figure 3.

Figure S3

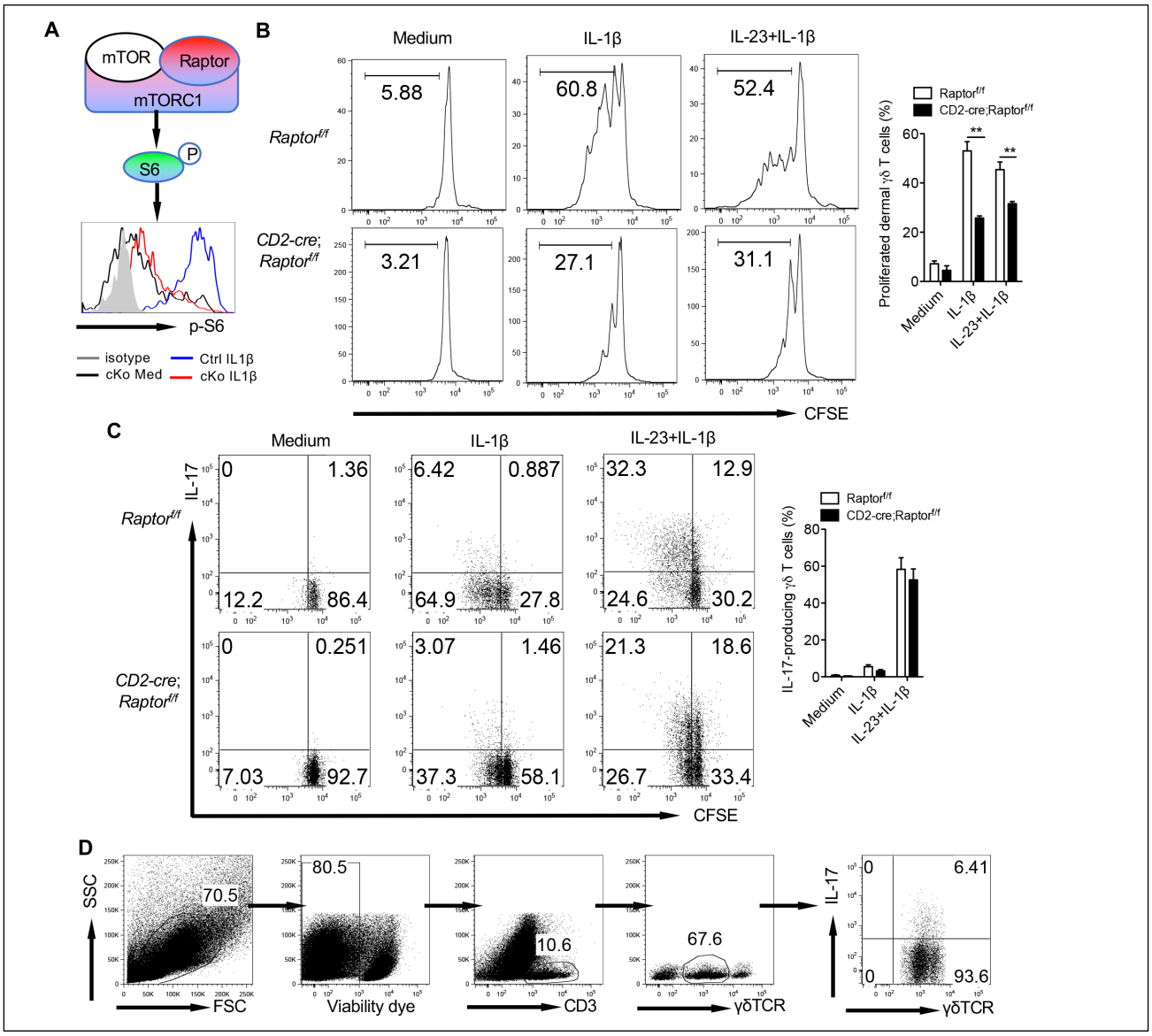

Figure S3. Roles of mTORC1 signaling in dermal γδT cell proliferation and IL-17 production. (A) Schematic of mTORC1 with representative histogram showing abolished mTORC1 activity (p-S6) in Raptor-deficient dermal γδ T cells upon IL-1β stimulation. (B, C) Whole skin cell suspensions from CD2-cre;Raptor$^{f/f}$ or control Raptor$^{f/f}$ mice (n=3-4) were labeled with CFSE and then stimulated with IL-1β or IL-23 plus IL-1β for 3 days. CFSE dilution (B) and intracellular IL-17 production (C) by dermal γδ T cells were determined by flow cytometry. Flow plots gated on CD3^{+}γδTCR^{Int} cells are representative of at least three independent experiments with similar results. Data are shown as mean ± SEM. **p < 0.01 (unpaired Student's t test). (D) Gating strategy for dermal γδ T cells and IL-17 production upon stimulation shown in Figure 3E. Related to Figure 3.

Figure S4

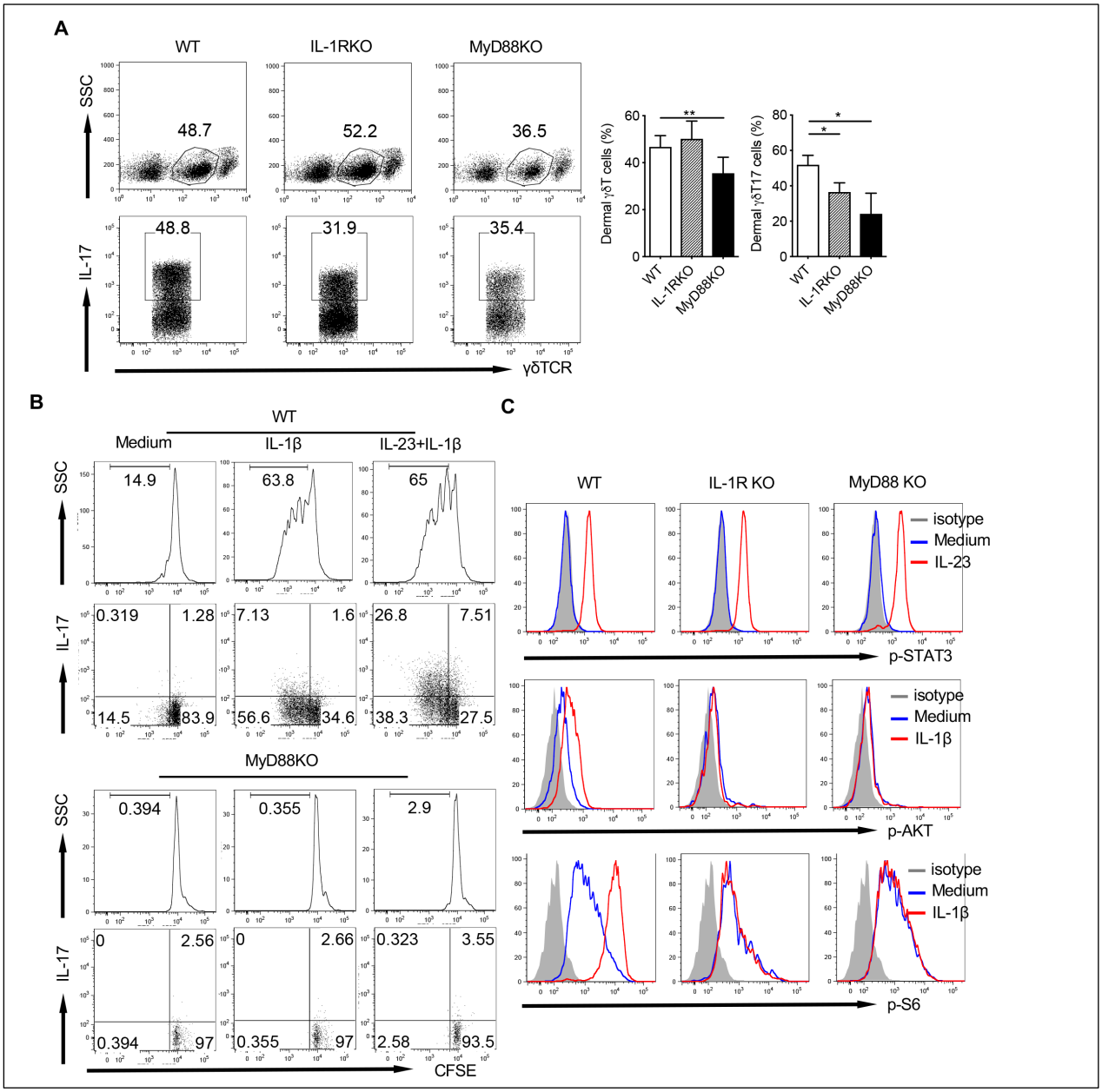

Figure S4. MyD88-mediated signaling pathway is essential in IL-1β-induced dermal γδT cell activation. (A) The frequency of dermal γδT cells (n=6) and the percentage of IL-17-producing γδT cells (n=3) after PMA plus ionomycin stimulation in C57BL/6 WT, IL-1R KO and MyD88 KO mice are shown. Flow plots gated on $CD3^+$ cells (top) or $CD3^+\gamma\delta TCR^{int}$ cells (bottom) are representative of two independent experiments with similar results. Data are shown as mean ± SD. *$p < 0.05$, **$p < 0.01$ (one-way ANOVA). (B) Whole skin cell suspensions from C57BL/6 WT or MyD88 KO mice were labeled with CFSE and then stimulated with IL-1β or IL-23 plus IL-1β for 3 days. CFSE dilution and intracellular IL-17 production by dermal γδ T cells were determined by flow cytometry. Flow plots gated on $CD3^+$ $\gamma\delta TCR^{int}$ cells are representative of at least three independent experiments with similar results. (C) Cultured skin γδ T cell lines from C57BL/6 WT, IL-1RKO and MyD88KO mice were stimulated with IL-23 or IL-1β for 30 minutes. p-Stat3, p-AKT and p-S6 were examined by flow cytometry. Flow plots gated on $CD3^+$ $\gamma\delta TCR^+$ cells are representative of at least two independent experiments with similar results. Plots from WT mice were the same shown in Figure 3B. Related to Figures 2 & 3.

Figure S5

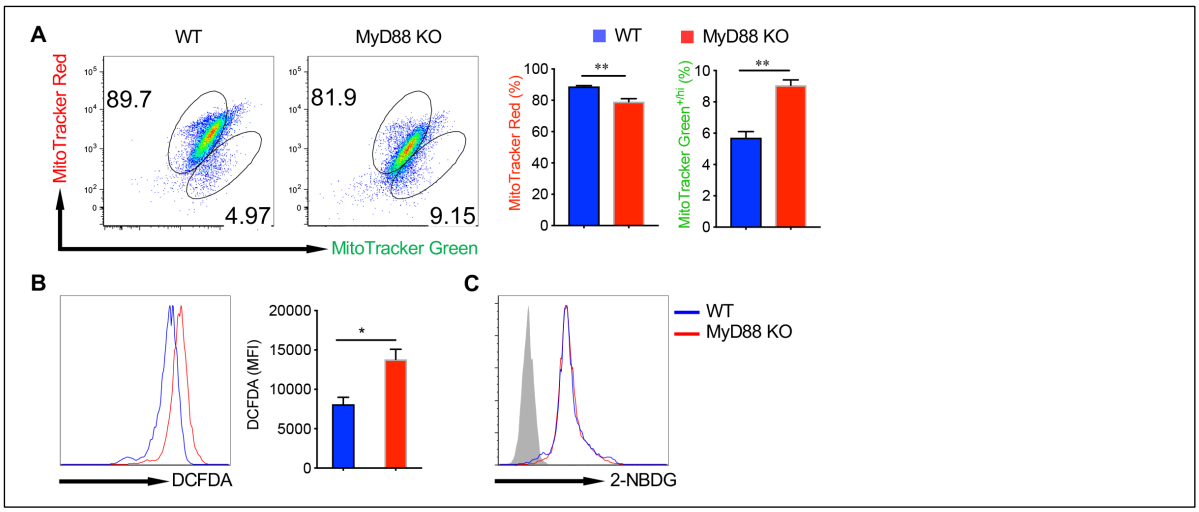

Figure S5. Reduced respiring mitochondria with enhanced ROS production in MyD88 KO dermal γδT cells. (A) Whole skin cell suspensions from WT and MyD88 KO mice (n=3) were stained with MitoTracker Green and MitoTracker Red. Percentages of MitoTracker Green$^{+/hi}$ and MitoTracker Red were analyzed by flow cytometry. Flow plots gated on CD3^{+}γδTCR^{int} cells are representative of two independent experiments with similar results. Percentages of MitoTracker Green$^{+/hi}$ and MitoTracker Red^{+} dermal γδT cells are shown as mean ± SEM. **p< 0.01 (unpaired Student's t test). (B, C) Whole skin cell suspensions from WT or MyD88 KO mice were stained with DCFDA (B) or 2-NBDG (C). Expressions of DCFDA and 2-NBDG were analyzed by flow cytometry. Flow histograms gated on CD3^{+}γδTCR^{int} cells are representative of two independent experiments with similar results. Summarized DCFDA MFI data are shown as mean ± SEM. *p<0.05, **p< 0.01(unpaired Student's t test). MFI: mean fluorescent intensity. Related to Figure 4.

Figure S6

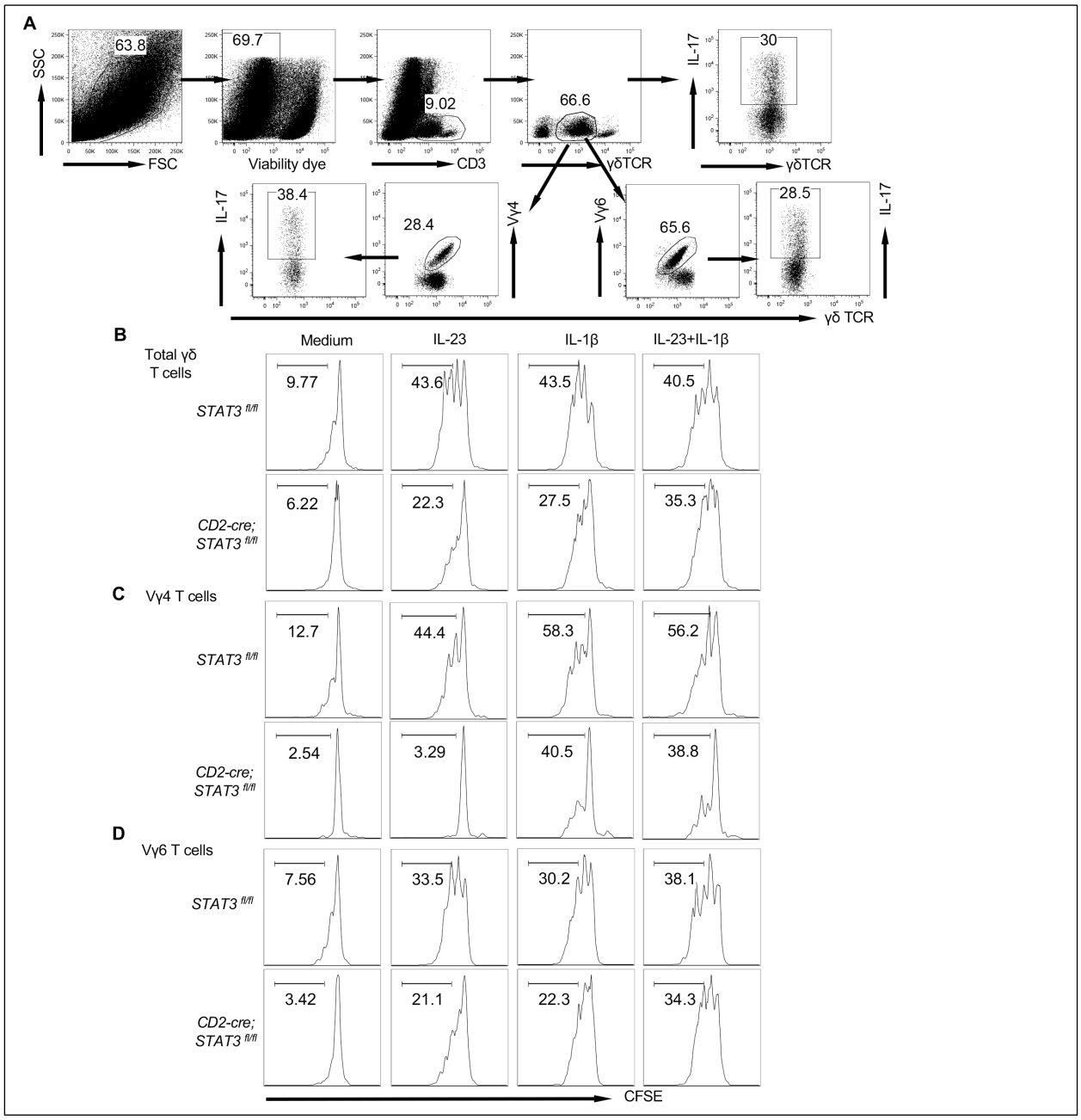

Figure S6. Roles of STAT3 signaling in dermal γδT cell proliferation. (A, B, C, D) Whole skin cell suspensions from CD2-cre;Stat3$^{f/f}$ or control Stat3$^{f/f}$ mice were labeled with CFSE and then stimulated with IL-1β, IL-23 or IL-23 plus IL-1β for 3 days. Gating strategy is shown (A). Dermal γδT cell proliferation (CFSE dilution) was determined by flow cytometry. Flow plots gated on CD3^{+}γδTCR^{int} cells (B), on CD3^{+}γδTCR^{int} Vγ4 (C), or Vγ6 (D) cells are representative of at least three independent experiments with similar results. Related to Figure 5.

Figure S7

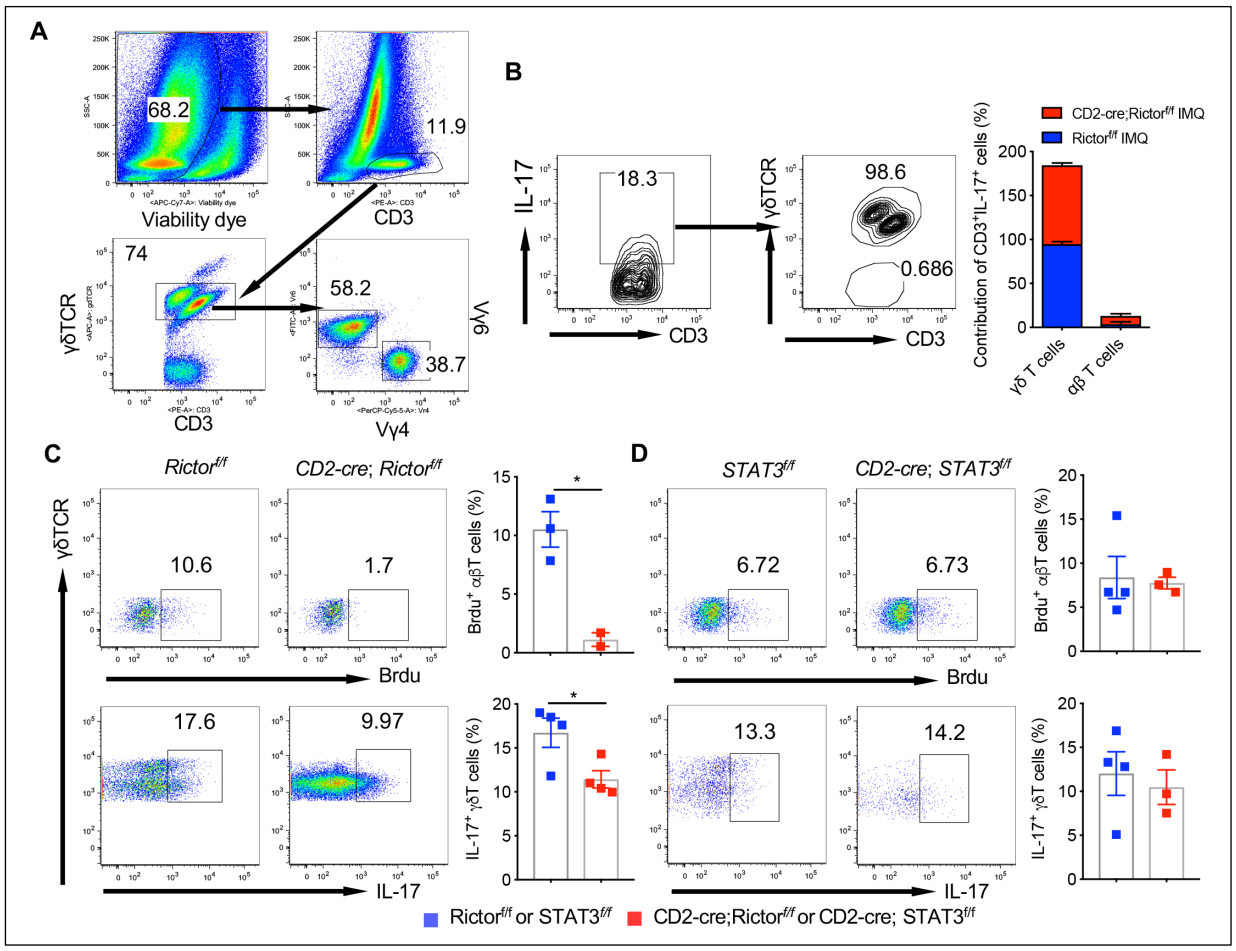

Figure S7. Dermal γδT cells are the major cellular source of IL-17 in the inflamed skin. (A) Gating strategy for dermal Vγ4 and Vγ6 T cells in control and Rictor cKO or STAT3 cKO mice treated with IMQ. (B) CD2-cre;Rictor$^{f/f}$ or control Rictor$^{f/f}$ mice (n=3) were treated daily for 5 days with IMQ or vehicle control. Single cells were stained for intracellular IL-17 without further stimulation. Flow plots were gated from CD3$^+$IL-17$^+$ cells first and percentages of CD3$^+$γδTCR$^-$ cells (αβ T cells) or CD3$^+$γδTCR^{int} (γδ T cells) were examined. Summarized data combined from three independent experiments are shown as mean ± SEM. (C, D) CD2-cre;Rictor$^{f/f}$ or control Rictor$^{f/f}$ mice (C) and CD2-cre;Stat3$^{f/f}$ or control Stat3$^{f/f}$ mice (D) were applied topically with IMQ for 5 days. Brdu were injected one day before mice were sacrificed. Skin single cell suspensions were stained for Brdu (gated on CD3$^+$γδTCR$^-$) and spontaneous IL-17 production without stimulation (gated on CD3$^+$γδTCR^{int}). Flow plots are representative of two independent experiments with similar results. Data are shown as mean ± SEM. *p<0.05, **p<0.01 (unpaired Student's t test). Related to Figure 7.